ACS Catalysis

Perspective

pubs.acs.org/acscatalysis

Metal Redispersion Strategies for Recycling of Supported Metal Catalysts: A Perspective

Kevin Morgan,* Alexandre Goguet, and Christopher Hardacre*

CenTACat, School of Chemistry and Chemical Engineering, Queen's University Belfast, David Keir Building, Stranmillis Road, Belfast, BT9 5AG, United Kingdom

ABSTRACT: Catalyst deactivation is ultimately inevitable, and one of the processes known to cause deactivation is sintering of metal particles. Consequently, numerous methods to reverse the sintering process by redispersing metal nanoparticles have been developed. These methods are discussed in this perspective, and the reported mechanisms of redispersion are summarized. Additionally, the longer-term practical use of such treatments and the benefits this can bring are briefly disclosed.

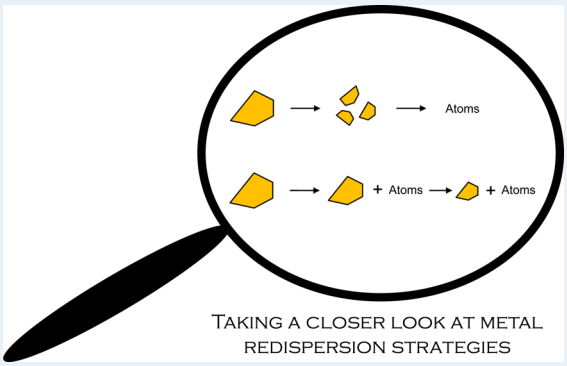

KEYWORDS: *catalyst recycling, catalyst regeneration, metal redispersion, catalyst deactivation, supported metal catalysts*

1. INTRODUCTION

In the field of heterogeneous catalysis, it is well documented that deactivation of catalysts is not only problematic, but also eventually inevitable.[1−3] Such deactivations can be as a result of both chemical and physical changes, and in the case of metal-supported catalysts, this can occur by way of a number of mechanisms, such as poisoning, coking, and sintering/agglomeration of metal nanoparticles.[1,2] Process technology considerations often mean that methods of reversing catalyst deactivations are developed. These can occur either during process operation (e.g., only a change of feed is required) or during a separate regeneration process (in which multiple conditions may need to be varied).[3]

To fully assess deactivation and reactivation due to changes in metal dispersions, one has to be mindful of the limitations of physico−chemical techniques (such as chemisorption, ultraviolet (UV), transmission electron microscopy (TEM) and X-ray based methods) that are used for such analysis. For example, chemisorption techniques assess particle size on the basis of adsorption. This is subject to error because the adsorption provides a measure of the surface area, and from this, a particle size is inferred on the basis of a number of assumptions, for example, the shape of the particle and the geometry of the adsorbed molecule on the surface. Similarly, it is known that the electrons generated in techniques such as TEM have the ability to change metal dispersions; hence, the best practice is to use a combination of techniques, including, where possible, synchronous characterization methods. There have been many reports of such studies combining, for instance, numerous spectroscopic techniques. Recently, the emergence of pair distribution function (PDF) to be utilized with traditional X-ray adsorption spectroscopy (XAS) and X-ray diffraction (XRD) studies has also been discussed.[4] In the future, the use of computed tomography with experimental techniques, such as XRD-PDF,[5] may prove to be very useful, given the ability to determine structural changes of "minor" components,[6] such as smaller metallic nanoparticles.

Catalytic activity and durability are often inversely proportional to the diameter of the supported metal particles, with smaller particles typically resulting in higher activities.[7,8] Consequently, the activity of supported metal catalysts is highly dependent on metal particle size.[9] For instance, for gold, the highest activity observed for CO oxidation was with gold particles 2−3 nm in diameter, whereas other reactions have their own optimum gold particle size.[10,11] However, it is also worth noting that in the case of gold, changes in electronic properties due to decreasing particle size (and lower coordination) can increase gold's ability to adsorb small molecules.[12]

The driving force for sintering is the thermodynamic instability of small crystallite particles (nanometers range), which possess a high surface-to-volume ratio.[13] This driving force increases exponentially with decreasing particle size;[14] that is, the greater the instability of the particles, the greater the driving force is for sintering.[15] Hence, larger metal particles are formed by the aggregation of smaller particles, meaning that the total accessible metallic surface is significantly reduced.[16] In some instances, preventive measures have been taken in the catalyst synthesis steps, but these may only delay the deactivation. For instance, the use of "capping agents", which

Received: March 13, 2015
Revised: April 21, 2015
Published: April 23, 2015

DOI: 10.1021/acscatal.5b00535
ACS Catal. 2015, 5, 3430−3445

are designed to protect against agglomeration, only delay the growth of the nanoparticles,[17] and hence, deactivation will still ultimately follow. An example of this is the use of Re to retard Pt sintering as it results in the dispersion to smaller aggregates, thereby increasing the catalyst lifetime before regeneration is required.[18] It has also been reported that the presence of Re can, in fact, restrict Pt migration and, thereby, limit sintering.[19−21] A similar restriction in Pt sintering as a result of addition of Sn has also been reported,[22] and this is thought to be a result of Sn poisoning acidic sites of the support,[23] although alloying with Sn is also reported to inhibit the Pt activity. A similar inhibition of sintering has been reported when Ir/Al_2O_3 was impregnated with CaO, SrO, or BaO, although the concentration of these metals (Ca, Sr, or Ba) must be higher than the concentration of the acid sites.[24] It is also noteworthy that addition of BaO to a sintered Ir/Al_2O_3 and subsequent oxidation (in air at 600 °C) caused the Ir metal to redisperse.[24]

The use of ligands (e.g., thiols) that can form strong sulfur−metal bonds (for instance, with Au and Pt) can stabilize mobile metal atoms on a CuO surface, resulting in highly dispersed metal particles upon removal of the ligands.[7] For example, tris(phenylthio)benzene (TPB) was adsorbed on gold nanoparticles, resulting in a decrease in the gold particle size from ∼4 to ∼1.5 nm. This was thought to be due to the TPB affecting the migration of the gold particles on the oxide, resulting in a change in particle size distribution. Additionally, when core−shell structures were prepared, it was suggested that the encapsulated nanoparticles were more resistant to sintering,[25−28] and this is a possible explanation for catalytic activity being maintained.[29]

Another synthesis method that has the potential to limit sintering and promote dispersion of metals (including Cu, Pt, and Pd) is the use of a support of a solid solution of mixed oxides containing at least one reducible metal oxide, such as ceria.[30−33] The presence of the reducible metal oxide facilitates the creation of metal−metal oxide interfaces under reducing conditions, which allows for the metal to be redispersed under oxidizing conditions.

Another possible route to prevent aggregation of nanoparticles is in the utilization of strong metal oxide/support interactions (SMOI or SMSI). It has been suggested that strong adhesion energy of nanoparticles of metal (Ag, Ir, and other late transition metals) to supports (including ceria, magnesia, and perovskites) is responsible for their resistance to sintering.[34,35] Obviously, SMSI effects are both metal- and support-dependent, so one can consider the thermal stability of the metal as a guide to this. For example, over Al_2O_3 and in an O_2 environment, the SMSI effect decreases in the order Rh > Pt > Ir > Ru, whereas in an in H_2 environment, the trend is Ir ∼ Ru > Rh > Pt.[36] In addition to this, it has been reported that the use of nonreducible metal oxides (SiO_2, Al_2O_3, MgO) as supports can stabilize very small particles, specifically gold.[37] More recent work has reported a new type of SMSI for Pt nanoparticles on ceria,[38] in which the Pt (as Pt_8) has been observed as a fluxional system in which the charge distribution and geometry are able to change, thereby facilitating an enhancement of catalytic activity.

Another factor to be considered is the role of the support in the redispersion process.[39] For instance, it has been reported that Pt supported on zeolite HY is much more prone to sintering than Pt/Al_2O_3 catalysts.[40] The ability to disperse Pt over a range of metal oxide supports (TiO_2, SnO_2, NbO_2, ZrO_2, SiO_2, Ta_2O_5, and Nb_2O_5) in low-temperature fuel cells (under the operating conditions of a polymer electrolyte membrane fuel cell (PEMFC) cathode) has also been reported.[39] Since Pt redispersion is considered an activated process, it was calculated that under such conditions, only NbO_2 was suitable for Pt redispersion in the desired potential interval, although SnO_2 also has some promise. This process is also affected by the acidity of the support. For example, using oxidative treatments (at 550 °C), increased Pt dispersion was observed in the case of acidic supports (Al_2O_3 and MgO), but decreased over basic/neutral supports (SiO_2, silica−alumina, silicalite).[41]

Despite attempts to prevent sintering, eventually, metal particles will sinter, resulting in deactivation of the catalyst. This is problematic, and as a result, some precious metal catalysts (particularly for automotive uses) tend to be loaded with excess metal to enhance the lifetime.[42] For instance, in automotive catalysts, the monoliths could contain as much as 2000 g t^{-1} of metal. This excess loading is to ensure that the catalyst remains effective even at the end of its guaranteed lifetime to comply with the environmental legislation.[43] Conversely, the demands on precious metal resources are ever-growing because of increased industrialization and legislation concerning emissions[42] Therefore, ways that can be developed resulting in the regeneration of catalysts through the redispersion of supported metals in sintered catalysts are critical for the future of emission control and chemical industries.

2. METAL REDISPERSION STRATEGIES

With catalyst deactivation comes the obvious pursuit of catalyst reactivation/recycling. In the case of deactivation by sintering, this will require the rejuvenation of the metallic sites. The regeneration process whereby the original metal dispersion of a sintered catalyst is achieved or even improved upon is known as "redispersion".[16] It is possible to regain or even improve upon the original dispersion, and in most cases, with this ability to redisperse the metal particles comes the ability to recover the catalytic activity. Note, however, that this will not always result in the original activity being recovered.[44]

The use of redispersion of metal nanoparticles in the reversal of sintering has existed almost from the point that sintering was identified as a deactivation process.[45] It has been argued that sintering and redispersion are two sides to the same process, which have a dependence on both temperature and atmosphere.[46] It has also been postulated that redispersion is in itself actually part of the sintering mechanism, whereby the metallic atoms become initially liberated from larger particles.[47] Hence, if the process is halted abruptly (normally by cooling), this dispersion will be maintained or frozen. There is some evidence that this does occur because it has been reported that catalysts that were rapidly cooled retained a higher dispersion than those allowed to cool slowly, in what was referred to as a "freezing of agglomeration".[48]

The ability to redisperse a metal is dependent on a number of factors, including temperature; redox environment; interaction between the metal and the support, which affects the activation energy of atom moving from metal nanoparticle to the support;[47] and the surface area of the support. It has also been reported (from Monte Carlo simulations) that the greater the initial particle size, the slower the redispersion process.[49] Similarly, the higher the initial metal content, then the more difficult it will be to redisperse the metal.[49,45]

Numerous redispersion strategies have been utilized for a wide range of metals (e.g., Pt, Au and Ag) and these are

DOI: 10.1021/acscatal.5b00535
ACS Catal. 2015, 5, 3430−3445

discussed in the subsequent sections. The strategies for metal redispersion are summarized in Table 1.

Table 1. Summary of References for Metal Redispersion Strategies

strategy	metals	references
oxidation and reduction	Fe	73−75
	Pt	16, 22, 40, 76−93
	Pd	94−107
	Rh	18, 79, 108−112
	Ag	113−119
	Au	10, 37, 120
	other metals and bimetallics	16, 18, 22, 79, 80, 121−123
chlorination and oxychlorination	Pt	19, 44, 50, 84, 158−170
	Pd	171, 172
	other metals and bimetallics	18, 19, 22, 79, 80, 169, 173−184
thermal treatment with iodomethane	Au	9, 188−190, 192−194
	Rh	191
treatment with halohydrocarbons other than iodomethane	Au	9

2.1. Oxidation and Reduction. One of the most common approaches to redispersion is techniques using cycles of oxidation and reduction, primarily with oxygen and hydrogen, respectively.[51] Such techniques are commonly used in industry, as indicated by the number of patents related to oxidation or reduction methods for catalyst regeneration, for example references 52−71, although not all of these refer to redispersion. During oxidation/reduction redispersion processes, it has been proposed that oxidations result in metal oxide particles, followed by mobilization of these particles. Thereafter, heated hydrogen treatments (typically short in duration) form the catalytically active metal particles through the reduction of the metal oxide. Short time scales for this process are necessary because sintering can occur after prolonged heating, particularly in reducing environments, although sintering can also occur while heating under oxidizing atmospheres.[72]

The temperature of such treatments dictates the ability to redisperse or sinter the metal.[73−75] For instance, in the case of iron on titanium oxide, reductive treatments (Fe^{3+} being reduced to Fe^{2+})[74] below 370 °C result in particles <10 nm (as observed via TEM);[73] however, in the temperature range of 404−434 °C, the Fe particles have been reported to grow to >10 nm.[73] Reductions at 500 °C resulted in Fe particles ∼10 nm in size, whereas reductions in the temperature range of 602−700 °C gave Fe particles that were ≤10 nm.[73] In these instances, the active catalyst is actually a mixed oxide of Fe and Ti, which is formed via oxidation at 677 °C, where a high iron dispersion is still maintained in the form of $FeTi_2O_5$ species. It should be noted that the first oxidation could not completely reverse the changes caused by the first reduction; neither were subsequent reductions found to completely reverse the effect of the corresponding oxidation step, reportedly a consequence of SMSI.[75] Such SMSI and temperature dependencies for the sintering/redispersion (and reversibility thereof) will be metal and support specific.

It should be noted that oxidation may not always result in redispersion to smaller particles. For instance, in the case of Pt, the oxidation process is thought to disrupt the metal lattice. When these particles are subsequently reduced, fissures appear in the Pt particles,[76] which can result in a higher Pt surface area, even though the Pt particle size remains apparently relatively unchanged. For this reason, one should not use chemisorption experiments alone to assess the extent of redispersion because any increase in Pt surface area will result in increased chemisorption as a result of the porosity changes. Therefore, any link between a change in H/Pt ratio (from chemisorption) and sintering/redispersion in the absence of further characterization is the subject of some debate.[77] Hence, it is preferable to make use of a combination of additional techniques to definitively monitor changes in metallic particle size (e.g., TEM).

2.1.1. Platinum. The ability to redispserse platinum over a range of supports with oxidation−reduction cycles has been well documented in the literature; however, it should be noted that it can take numerous cycles of oxidation−reduction before any redispersion is actually observed.[78] The effect of oxidation−reduction cycles on Pt/Al_2O_3 catalysts has been examined through activity studies[18,22] and using CO adsorption IR spectroscopy.[79,80] Interestingly, it was also found that repeated oxidation cycles actually resulted in Pt sintering.[22]

TEM studies have shown that the redispersion of Pt particles was observed from 10.7 to 4.1 nm after heating a $Pt/\gamma\text{-}Al_2O_3$ catalyst in air at 600 °C for 18 h, followed by heating at 500 °C, also in air, for a further 18 h.[81] Prior to analysis with TEM, the samples were immersed in mercuric chloride and then rinsed with water before being stored under high vacuum for several hours to avoid any contamination of the microscope. There was no apparent reduction treatment, although the storage under high vacuum for several hours would have created a significant reducing environment. Some redispersion was achieved at lower temperatures (400 °C) following the 600 °C treatment, but to a lesser extent than that observed after heating at 500 °C.[81]

A different study reported an optimum temperature for redispersion of Pt (in the case of a number of prereduced Pt/Al_2O_3 catalysts).[82] In this case, oxidation at temperatures up to 600 °C, followed by a reduction with H_2 at 500 °C, resulted in dispersion of the Pt (30%) that was higher than that obtained with the fresh catalyst (10%). However, the maximum dispersion was observed after oxidation at 550 °C (70%), and sintering began to occur again at temperatures greater than this. This optimum temperature has been reported elsewhere for oxidation−reduction cycles, and highly dispersed metallic particles have been observed after reduction at 550 °C.[40] It was actually reported in this instance that the redispersed Pt was resistant to any subsequent sintering.[40] It should be noted, however, that there are also reports in the literature of original dispersions of fresh catalysts being restored at 480 °C.[83]

XRD and TEM were used to study the hydrogen storage capacity of a range of Pt/MgO catalysts as a mean to assess changes in Pt particle size after oxidation and reduction.[84] It was found that oxidative treatments between 550 and 800 °C resulted in Pt particles with a reduced average crystallite size.

Using a cyclic oxidative/reductive process, it was found that at all studied temperatures (500−800 °C), the particle sizes of Pt were smaller after the oxidation step (2.21−9.56 nm) compared with the Pt particle size after the reduction (3.03−11.11 nm), although the particle size even after reduction was still smaller than that observed for the fresh catalyst.[16] Similar trends were noted in other studies of the same monometallic Pt

DOI: 10.1021/acscatal.5b00535
ACS Catal. 2015, 5, 3430−3445

catalyst.[85] It should, however, be noted that this was quite a prolonged reduction step (16 h at 150 °C and 2 h at 250 °C) in pure hydrogen. Consequently, the fact that some sintering occurred during this reduction step is not surprising. Therefore, as previously stated in this Perspective, it is important that any reductive step conducted after oxidations is done under carefully controlled conditions.

XRD, TEM, X-ray adsorption fine structure (XAFS) and X-ray photoelectron spectroscopy (XPS) have all been employed to study the sintering and redispersion of Pt in Pt/MgO and Pt/γ-Al_2O_3 catalysts.[86] Therein, the catalysts were aged at temperature (700, 800, and 900 °C) for 5 h in two ways: in constant air flow (air aging) or in a flow switching every 5 min between 5% O_2 in N_2 and 10% H_2 in N_2 (redox aging). Activity tests with simulated exhaust gas (0.7% CO, 0.23% H_2, 0.053% C_3H_6, 0.12% NO, 0.646% O_2, 10% CO_2, and 3% H_2O in N_2) reactions were then conducted with the aged catalysts, with conversion of CO, C_3H_6, and NO_x monitored.

The air aging tests had little effect on the activity of the Pt/MgO, but caused a significant decrease in the activity of the Pt/γ-Al_2O_3. Hence, Pt/MgO was more stable under high temperature oxidative conditions than Pt/γ-Al_2O_3. An explanation for this was that no sintering of Pt occurred on Pt/MgO, but Pt particles as large as 30 nm formed on the air aged Pt/ γ-Al_2O_3 catalyst.

It was previously demonstrated that the interaction of Pt with the support oxide occurs under oxidizing conditions and that the inhibiting sintering effect on Pt can be controlled by support oxygen electron density through the interaction of Pt oxide with the support.[87] The formation of Mg_2PtO_4 compounds during the air aging process is thought to inhibit Pt sintering, thereby explaining the stability of Pt/MgO under high-temperature oxidizing conditions. This is in agreement with previous studies that showed that the Pt interactions with alumina were much weaker,[87] thus explaining the lack of Pt redispersion in Pt/γ-Al_2O_3.

The redox aging tests were found to have an adverse effect on the activity of both the Pt/MgO and Pt/γ-Al_2O_3 catalysts for simulated exhaust reactions. It was observed that the Pt particle size had grown for both Pt/MgO (15−25 nm) and Pt/γ-Al_2O_3 (20−30 nm) following the redox aging tests. It was determined that the deactivated Pt/MgO catalyst could be regenerated by redispersing the Pt nanoparticles, following a process of sequential treatments involving 20% O_2/N_2 for 5 h and then 10% H_2/N_2 for 5 h at 800 °C. However, under the same conditions, the activity of the Pt/γ-Al_2O_3 continued to decrease. Consequently, it was reported that the formation of Mg_2PtO_4 was the driving force of the redispersion process. This is further evidence that a strong metal support interaction is desirable for catalyst regeneration via redox treatments, at least in the case of Pt.

Similar conclusions were drawn when a Pt/Al_2O_3 catalyst was compared with a Pt/CeZrY mixed oxide catalyst using in situ time-resolved Turbo-XAS.[88] For the Pt/Al_2O_3 catalyst, it was observed that as temperature increased, so too did the Pt particle size (>20 nm); it was also noted that the particle size did not decrease again upon cooling. However, in the case of Pt/CeZrY mixed oxide, the particle size increased from 1.8 nm for the untreated catalyst to 4.4 nm as the temperature was increased from 400 to 800 °C, whereas particle size decreased again to 2.7 nm when cooled to 550 °C. Hence, this sintering/redispersion could be controlled reversibly by temperature. Again, the strong interactions between Pt oxide and the support (primarily ceria) was thought to be the reason for the redispersion process.

The nature of the Pt redispersion was further studied in terms of how the initial Pt particle size affected the rate of Pt redispersion.[88] It was determined that the larger the initial particle size, the slower the redispersion process, in agreement with Monte Carlo simulations.[49]

The effect of temperature on the rate of redispersion was also investigated.[88] Not surprisingly, the redispersion occurs faster at higher temperatures, indicating an activated process, a fact that is reinforced considering no redispersion occurred at 400 °C or below. Additionally, it was found that redispersion occurred much faster at higher oxygen concentrations, which supports the theory that Pt oxide interactions with the support are important to the redispersion process.

It has been reported that the agglomeration of Pt can occur in both reducing and oxidizing atmospheres, particularly at temperatures above which Pt^{2+} species typically decompose.[89] However, subsequent oxidation at lower temperatures results in a mobile PtO phase, which can result in highly dispersed metallic particles after a controlled reduction.

In general, it has been reported that Pt dispersions of Pt/Al_2O_3 catalysts after treatment with oxygen are higher than the dispersions found after hydrogen treatments.[90] It has been reported that when increasing oxygen concentration during oxidative treatments of a Pt/Al_2O_3 catalyst, PtO forms, which promotes the formation of Pt−Al_2O_3 complexes and subsequent migration of Pt species into the bulk lattice of the support.[91] Upon reduction, these PtO and Pt−Al_2O_3 species form Pt metal, resulting in a greater Pt dispersion being observed. However, it has also been reported that heating in oxygen can cause catalyst deactivation, whereas heating in hydrogen (or nitrogen) resulted in activation (at temperatures >400 °C) for the hydrogenation of cyclohexane and decomposition of hydrogen peroxide.[92] At temperatures below 400 °C (for all atmospheres), sintering and deactivation occurred. At higher temperatures in hydrogen (and to a lesser extent, nitrogen), oxygen is removed from the surface of the support, which in fact promotes dissociation of Pt crystallites and surface mobility of the Pt, toward these vacancies.[92] A similar mechanism (and trends; sintering in oxidizing and redispersion in reducing conditions) has also been proposed for a Pt/TiO_2 catalyst.[93] In this case, a change in the titania was observed (from TiO_2 to Ti_4O_7) as a result of the reduction of the surface removing oxygen and creation of vacancies.[93] In this case, the Pt metal is thought to interact with exposed Ti cations to form Pt−Ti bonds, which rupture under oxidizing conditions, reforming the TiO_2 and causing Pt agglomeration.[93]

2.1.2. Palladium. Previously, the dependency of catalytic activity on the Pd particle size has been observed under CO/NO cycling.[94−96] Therein, from the CO/NO cycling experiments, it was reported that an increased size of Pd nanoparticles was found to have a negative effect on the production of CO_2. In a study using EXAFS, DRIFTS, and MS of NO reduction/CO removal, it has been reported that rapid, reversible sintering and a novel, nonoxidative redispersion of Pd nanoparticles occurred during cycles between CO and NO flows.[97] This occurred without chlorine present and without significant Pd oxidation. Experiments were conducted at 400 °C on a 1 wt % Pd supported on 10% ceria−zirconia on alumina (10ZCA) catalyst, cycling between flows of 5% CO/He and 5% NO/He. Although the fresh catalyst was found to contain PdO nanoparticles almost exclusively, in both the CO

DOI: 10.1021/acscatal.5b00535
ACS Catal. 2015, 5, 3430−3445

and NO environments, there was no PdO detected, and the Pd−Pd bond lengths observed were characteristic of metallic Pd and Pd nanoparticles. However, the Pd−Pd coordination was higher in the CO environment than in the NO environment, with particles of ∼100 Pd atoms forming due to sintering by CO. Under the NO environment, nonoxidative dispersion of these large particles occurred, resulting in particles of ∼20−25 Pd atoms. The sintering/redispersion mechanism involved removal of adsorbed oxygen from the fresh catalyst by CO (reductant). Once the adsorbed oxygen was depleted, the sintering of the Pd occurred in tandem with the CO adsorbing on metallic Pd, as observed with IR spectroscopy. Under the NO feed, the adsorbed CO was removed from the surface, and Pd redispersion occurred, most likely, by a combination of both particle splitting and flattening.[97]

Extended X-ray adsorption fine structure (EXAFS) studies were also conducted on a chloride free Pd/Al_2O_3 catalyst during redox cycles with CO as the reductant and NO as the oxidant both in the absence and presence of oxygen.[98,99] The overall observed trend was the same during the CO/NO cycles as that discussed previously,[97] that is, sintering in CO and redispersing in NO. However, in the presence of O_2 during the NO cycle, the amount of redispersion achieved was found to significantly increase, although this occurred without oxidation of Pd.[98,99] The postulated mechanism involves an initiation step of significant Pd redispersion prior to the formation of the more stable PdO[98,99] that, as already discussed, can migrate further over the support, ultimately resulting in a higher metallic dispersion upon reduction.

A similar observation has been made for Pd supported on perovskite used in catalytic convertors.[100] Samples were cycled between lean (oxidative) and rich (reductive) engine conditions at 800 °C using a sequence of oxidation (in air for 1 h), reduction (10% H_2 for 1 h), and reoxidation (in air for 1 h). It was reported that the oxidation−reduction−oxidation cycle caused Pd migration in and out of the lattice of the perovskite, hindering sintering of Pd. This provided an explanation for the longevity of these catalysts due to apparent "self-regeneration", as has been previously reported.[42] Crucially, with a refined methodology, the perovskite material was also found to be equally effective in promoting self-regeneration in Pt and Rh as well as in Pd.[101] It is also noteworthy that these self-regenerating catalysts have been utilized in nonautomotive applications, such as organic reactions, including Suzuki coupling.[102,103]

2.1.3. Rhodium. While studying CO hydrogenation using Rh catalysts ($RhVO_4/SiO_2$, Rh/SiO_2 and V_2O_5−Rh/SiO_2), the mean sizes of the Rh particles was assessed.[104] After reduction (at 500 °C), it was found that the Rh precursors used for catalyst preparation decomposed to form highly dispersed Rh particles, the size of which varied for $RhVO_4/SiO_2$ (4 nm), Rh/SiO_2 (9−10 nm), and V_2O_5−Rh/SiO_2 (9−10 nm). It was further determined that, after reaction, when the catalyst was sintered, it was possible to regenerate the rhodium vanadate complexes via oxidation at 700 °C and then recover the highly dispersed Rh through a subsequent reduction step.

High-resolution electron microscopy (HREM) studies looked at the influence of reduction/reoxidation conditions on the particle size distribution of a series of Rh/CeO_2 catalysts prepared from $Rh(NO_3)_3$ and $RhCl_3$.[105] Reductions and reoxidations were conducted using a flow of H_2 or O_2 while heating the catalyst from 25 °C up to selected reduction temperatures (350, 500, and 900 °C) at a rate of 10 °C min^{-1} before dwelling for 1 h. Reduction at 700 °C and reoxidation at 800 °C were also investigated. Progressive sintering was observed during reduction up to 700 °C, and significant sintering occurred at 900 °C. Rh redispersion was observed only during the reoxidation treatments at 800 and 900 °C, whereas the reoxidation at 500 °C induced sintering. In previous studies[106,107] employing TPO experiments, it was determined that both the metallic and oxidized Rh phases were present following reoxidation treatments at lower temperatures (100 and 250 °C); however, polycrystalline Rh_2O_3 particles were found to be the almost exclusive phase after reoxidation at 500 °C. Reoxidation at higher temperatures was found to encourage the migration of these Rh_2O_3 particles across the CeO_2, which then could be reduced to highly dispersed metallic Rh.

2.1.4. Rhenium. For a Re/Al_2O_3 catalyst studied using chemisorption, electron spin resonance (ESR) and temperature programmed reduction (TPR), a dispersed oxide phase had a high level of interaction with the support, which readily reduced to metallic Re at temperatures >500 °C while maintaining dispersion.[108] The crystallite oxide phase could be oxidized further to Re^{7+} and then subsequently reduced to metal Re in hydrogen at 350 °C. This metallic Re could be dispersed via oxidation, followed by exposure to vacuum or inert gas at 500 °C. This dispersed oxide phase could then be reduced to Re metal, as mentioned previously.[108] Such characteristics (spreading of oxide phase and reduction of oxide) have been further confirmed by similar experiments using XPS.[109]

The Re dispersion of 1 and 10 wt % Re/γ-Al_2O_3 catalysts following four different oxidation−reduction treatments was monitored using hydrogen chemisorption, TEM, XRD, electron diffraction and electron spin resonance,[110] and in terms of the activity and selectivity of the catalysts for hydrogenation and hydrogenolysis of benzene.[111] The 1 wt % Re catalyst was subjected to 20 oxidation−reduction cycles, and 10 wt % Re catalyst underwent 10 oxidation−reduction cycles.

The chemisorption results of both 1 and 10 wt % Re/γ-Al_2O_3 indicated that surface area and Re dispersion increased relative to the untreated catalyst after oxidation at 400 °C. An increased dispersion was also noted for the catalysts stored in air at room temperature for several months, which undergo a low-temperature oxidation in this time. The Re dispersion increased only slightly after calcination of the long-term, low temperature oxidized catalyst. XRD and TEM were unable to satisfactorily detect the Re of 1 wt % Re/γ-Al_2O_3, and it was assumed that Re was highly dispersed in all the cases studied. No metallic Re was observed in the XRD and TEM of the passivated 10 wt % Re/γ-Al_2O_3, and it was concluded that Re was completely oxidized to Re_2O_7. After the reduction at 550 °C, metallic Re particles of ∼4 nm were observed with TEM as well as in the XRD. It was found that reoxidizing at 400 °C resulted in rhenium oxide again, and it was assumed that this was highly dispersed because it was not observed with TEM or XRD. After the subsequent reduction at 500 °C, Re was once again present in the metallic form (observed by TEM), but the particle size had decreased further (to ∼3 nm).[110]

From these results, two possible mechanisms (oxidation at low temperature and 400 °C) for the Re redispersion were proposed. At low temperatures, although the catalyst was stored in air, the Re slowly oxidized, resulting in hydrated rhenium oxide. This caused the Re_2O_7 clusters to split into smaller particles, which are mobile via surface diffusion. The reduction process then resulted in Re_2O_7 particles reducing to highly

DOI: 10.1021/acscatal.5b00535
ACS Catal. 2015, 5, 3430−3445

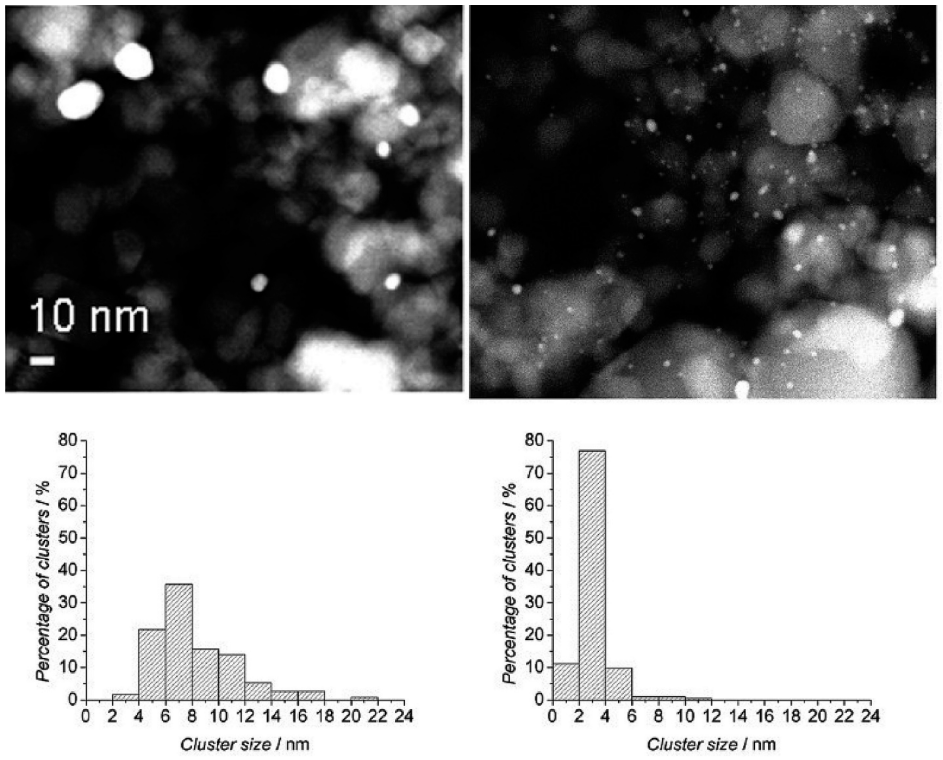

Figure 1. High-angle annular dark-field scanning transmission electron microscopy (HAADF-STEM) micrographs and particle size distributions of Au/TiO_2 catalysts treated in H_2 at 60 °C and then again after hydrogenation of 4-nitrobenzaldehyde at 100 °C and 10 bar H_2.[120]

dispersed metallic Re particles. The mechanism for the oxidation at 400 °C occurred through the formation of Re_2O_7, which has a low melting point and high vapor pressure, meaning that Re_2O_7 could migrate via the gas phase as well as through surface diffusion. Once again, subsequent reduction yielded metallic Re of a smaller particle size and uniform dispersion.[110]

This study also highlighted that the redispersion of the active metal is not always beneficial. For example, in the hydrogenolysis reaction, the dispersion of the Re that yielded the highest TOF was 26%, and the activity was found to decrease rapidly at higher dispersions. Furthermore, the selectivity during hydrogenolysis, although relatively constant (~60%) for dispersions up to 60%, was found to decrease at higher dispersions. The opposite trend was observed for the hydrogenation, in which selectivity was steady at 40−60% dispersion, before increasing up to 80% selectivity at higher dispersions. Importantly, it was found that the redispersion process did not result in any loss of Re.

In a follow-up study,[112] HRTEM, H_2 chemisorption, O_2 uptake, and XRD were utilized to further understand the mechanism of the oxidative redispersion process. In the proposed scheme for oxidation and redispersion, a number of temperature-dependent processes were proposed. At low temperatures (20−150 °C), superficial Re oxides (including Re_2O_7) are formed as a result of dissociative oxygen chemisorption. In the 200−250 °C range, oxidation and sublimation of Re occurs, with HRTEM showing that metallic Re particles were present, without any surface oxide layer. At 300 °C, complete oxidation of Re to Re_2O_7 occurs, with only small traces of metallic Re observed with HRTEM. Between 400 and 600 °C, surface compounds of ReO_4 form. These compounds decompose at 800 °C, with some sublimation to Re_2O_7. In the case of the sample oxidized at 500 °C, further reduction at 550 °C resulted in redispersion via the reduction of the surface compounds to small metallic Re particles.

In the studies of Re/Al_2O_3 catalysts under the conditions discussed previously[18,79] the Re dispersion increased (along with increased activity for the heptane-H_2 reactions) after oxidation at 550 °C; however, these catalysts were still prone to deactivation via coking.[18,79]

2.1.5. Silver. Changes in the morphology of Ag nanoclusters supported on titania due to oxygen have also been reported.[113] XPS and scanning tunnelling microscopy (STM) were used to observe the changes in Ag morphology following redox treatments. Initially, a unimodal Ag particle size distribution was observed (2.0−6.5 nm) for the untreated catalyst. Following oxidation of the catalyst, it was found that Ag_2O particles were formed in a bimodal size distribution with sizes of 1.0−5.0 nm and 5.0−11 nm. This meant that although some clusters became reduced in size, others increased. It was determined that the clusters that increased in size did so through Otswald ripening, a form of intercluster transport in which clusters grow at the expense of others. In this work, it was noted that under vacuum or reductive conditions, migration of Ag from clusters could occur only in the form of free metallic Ag atoms.[113]

It has also been observed with diffuse reflectance UV (DRUV), EXAFS, and UV−vis that even under mild reduction conditions,[114−116] including vacuum conditions,[117] silver has a tendency to aggregate. For instance, EXAFS showed that upon exposure to a selective catalytic reduction (SCR) mix, Ag^+ ions aggregate to form a range of active clusters of $Ag_n^{\delta+}$ (average n value of 3).[115] In XRD and EXAFS, study of similar $Ag/\gamma\text{-}Al_2O_3$ found that samples aged in the SCR reaction feeds between 600 and 800 °C underwent similar reconstruction.[118] After aging at

DOI: 10.1021/acscatal.5b00535
ACS Catal. 2015, 5, 3430−3445

600 °C, the Ag atoms coalesced into small clusters of ∼3 atoms. However, using the same feed conditions at 800 °C, the Ag−Ag coordination number began to decrease (from 3.2 to 2.1) as the larger particles began to redisperse to form smaller Ag clusters. These smaller clusters are thought to be a precursor to silver aluminate compounds.[119] The changes in Ag dispersion during the aging process had different effects on the SCR in the presence and in the absence of hydrogen. For instance, increased dispersion actually had an adverse effect on the activity of the hydrogen promoted SCR reactions, whereas in the absence of hydrogen, there was a promotional effect for the SCR reaction from the Ag reconstruction at 600 °C.

2.1.6. Gold. A DRIFTS, MS, and XRD study of a Au/CeO_2 catalyst used for CO oxidation has revealed the dependence of gold particle size on redox conditions.[10] The results indicated that during the reductive conditions of CO adsorption studies, the metal dispersion increased as the Au species became oxidized and diffused from the metal oxide bulk to the surface. This was attributed to Au−support interaction, the formation of $(O)Au^+$−CO species resulting from CO creating oxygen vacancies on the surface. These gold−ceria interactions promote migration of gold particles, resulting in redispersion of the gold through etching of the larger gold particles.[10]

Similar conclusions were also drawn from in situ XRD and Raman studies of Au supported on a cerium−europium mixed oxide used for the CO oxidation.[37] It was reported that doping with europium increased the number of oxygen vacancies, thereby promoting the ability of Au to diffuse through the support via stronger Au-support interactions. It was determined that the number of oxygen vacancies increased during reductive conditions (H_2), which resulted in increased gold dispersion. Oxidative treatments (in synthetic air), in which oxygen vacancies were replenished, make the Au−support interactions become less favorable than when under reducing conditions, causing Au particles to sinter. This sinter/redispersion process was found to be reversible because of its dependency on the existence of oxygen vacancies and, therefore, the oxidative/reductive nature of the environment.

During EXAFS, TEM, and SEM studies, Au/TiO_2 catalysts used for liquid phase hydrogenations were found to undergo redispersion from particles of 8 nm to smaller particles of 2−3 nm.[120] In contrast, larger particles (8−10 nm) formed during the reduction (H_2, 60−300 °C) of the fresh catalyst. After the liquid phase hydrogenation reactions, it was found that the average Au particle size decreased to ∼2−3 nm, and these particles were stable under reaction conditions. Such redispersions did not occur over Al_2O_3 support. Figure 1 reports a comparison of TEM and particle size distribution of an Au/TiO_2 reduced in hydrogen at 60 °C (on the left) and then this treated catalyst following the hydrogenation reaction, and the differences in particle size are clearly observed.

The proposed mechanism of the redispersion, in this case, involves Au interaction with oxygen vacancies of the support and the presence of H_2 (or reducing conditions) increasing the quantity of these vacancies, hence, promoting redispersion of the gold. This is in agreement with other studies in the literature.[10,37]

2.1.7. Other Metals and Bimetallic Catalyst Systems. The dependency of metal dispersion on oxidative and reductive treatments has also been observed for a Co/TiO_2 catalyst.[121] Reduction was found to generate smaller particle sizes at 700 °C than at lower temperatures. It was proposed that the Co particles are originally bound chemically to the oxygen of the support, and these bonds can be broken at higher temperature while a phase transformation from anatase to rutile proceeds, thereby causing the Co to redisperse.

The effect of oxidation and reduction cycles on $Pt−Sn/Al_2O_3$ has also been studied using pulsed CO chemisorption and IR spectroscopy,[22,80] as well as XRD.[80] The samples were first calcined in air during a 15 °C min^{-1} temperature ramp up to 400 °C (followed by a 30 min dwell), followed by reduction at 400 °C for 1 h in H_2. A series of six consecutive oxidation (1 h at 550 °C; 60 mL min^{-1} of air) and reduction (1 h at 400 °C; H_2) cycles were then employed.[22] The results indicated that the Sn partially hindered sintering of Pt, although the ability to redisperse the Pt via oxidation−reduction was also significantly diminished.

The deactivation and regeneration of a range of Pd/Rh monolith catalysts (removed from a commercial automobile exhaust gas system) using oxidation and reduction treatments at temperatures up to 500 °C has also been investigated.[122] TEM images of fresh samples, combined with EDX analysis, confirmed that no noble metal particles of size >3 nm were present on the monolith. In the aged samples, large agglomerates of metal were observed, including some Pt and Pd particles as large as 100 nm. TEM of aged samples after oxidation (10 h, 20% O_2 in N_2) showed a reduction in some of the agglomerates, and although activity in terms of HC and NO_x conversion were recovered, the authors pointed out that the removal of contaminants from the surface could also be a factor.

As mentioned previously, a pulse chemisorption technique has also been used to study Pt−Re bimetallic catalysts.[16] It was found that the bimetallic catalyst was more resilient to sintering than the monometallic Pt system. This was shown by the fact that, when the catalysts were sintered at 800 °C, only the bimetallic catalyst was catalytically active after redispersion. The bimetallic system was found to sinter in reducing environments and redisperse in oxidizing environments. It was concluded that the Re inhibited the sintering. It was further concluded that a temperature threshold existed below which metal−support interactions in the form of $PtO−Al_2O_3$ complexes did not occur, and it was above this temperature where redispersion could proceed.[16]

Similar studies on the oxidation−reduction cycles of $Pt−Re/Al_2O_3$ catalysts have been conducted using the conditions discussed previously.[18,79] In this case, trends in dispersion similar to those for the Pt/Al_2O_3 catalyst were observed (i.e., Pt sintering), indicating little effect of the Re, although evidence of formation of bimetallic particles was reported.[18,79]

While studying methanol carbonylation over Ir−La/C, it was found that the addition of La inhibited the deactivation of Ir catalysts, which occurred by sintering and reduction to metallic Ir.[123] With the Ir−La/C catalyst, it was observed that a greater dispersion of the metal(s) was achieved following an activation treatment in syngas (CO-to-H_2 ratio of 4:1), with particles being mostly 1−3 atoms in size. This high dispersion has been attributed to formation of Ir−La hydrocarbonyl species after exposure to CO) along with the role of La in stabilizing Ir and Ir^+ species.

2.1.8. Summary. Oxidation and reduction cycles have been reported to be successful in the redispersion of a number of metals. However, under certain conditions, this process has its limitations. For instance, it has been reported that the oxidation and reduction can be useful for redispersion, provided:[124]

DOI: 10.1021/acscatal.5b00535
ACS Catal. 2015, 5, 3430−3445

1. The metal can be oxidized under the conditions used, and
2. Reduction can occur without sintering (i.e, the sintering temperature is higher than the temperature for metal oxide decomposition)

It has also been stated that this process may not be ideal for metals forming oxides that are highly stable and highly mobile.[124] In instances where oxidation and reduction are found not to be ideal for the redispersion, it has been suggested that reduction after the formation of metal sulfides, carbides, or chlorides could be a viable alternative.[124] For instance, in the case of Pt on different supports, the metal can redisperse in O_2 only (at 600 °C) if the support is Al_2O_3.[125] If the support is TiO_2, chlorine (from CCl_4) was needed to enable redispersion.[125]

The mechanism of redispersion via oxidation/reduction cycles is in the form of the "strain" model[81] and can be summarized as follows:

- Oxidation causes the large metallic agglomerates to undergo oxidation
- Oxymetal species form on the surface of the particle
- The variation in metal−metal distances in the metal oxide surface layer and those in the unoxidized metal causes/induces a metal strain energy
- Oxymetal particles progressively fragment from the large particle (by fracture of the larger particle)
- Fragmented oxymetal species undergo dispersion through interactions with the support

2.2. Chlorination and Oxychlorination. The use of halogen species (primarily chlorine-based) to boost redispersion is commonplace and has been in existence for decades. Halogens are used widely for catalyst regeneration, as indicated by the number of patents related to such processes.[126−157] Although chlorine is primarily used for redispersion (and the discussion in this section will reflect this), it has also been reported that Br can be used for the redispersion of metals and, in particular, Pt on Al_2O_3.[44]

2.2.1. Platinum. It has been reported that the rate of Pt redispersion was greatly increased in the presence of chlorine species,[84] and total metallic dispersion has been reported when small concentrations (0.9−1.0%) of chloride have been utilized.[158] Interestingly, the use of halogenated precursors (e.g., aqueous H_2PtCl_6) for the preparation of a catalyst can result in an initially higher Pt dispersion than if a non-halogenated precursor (acetone solution of $Pt(C_5H_7O_2)_2$) is used.[84,159] Residual chlorine from the precursor can form HCl vapor under reaction conditions and increase the dispersion/accessibility of the metal (specifically Pt in the reported case).[160] This is also the case when a catalyst has been chlorinated after preparation.[159] It has been proposed that chlorine inhibits growth of Pt (on alumina)[159] and stabilizes Pt,[50] thereby increasing its ability to be dispersed.[50]

Pt/Al_2O_3 catalysts have been monitored under oxygen and hydrogen treatments for redispersion[161] and sintering[162] using TPR and UV−vis, respectively. Three samples of highly dispersed Pt catalysts supported on alumina were studied, including one that had been chlorinated. Redispersion during oxygen treatment was observed only in the presence of chloride, a process that was associated with an oxychloroplatinum surface complex species, $Pt^{IV}O_xCl_y$, the existence of which was confirmed by TPR.[161] The presence of this complex was also confirmed with UV−vis in the redispersed catalysts prior to sintering.[162] The Pt redispersion process on pre chlorided Pt/Al_2O_3 catalysts has also been investigated in IR studies[163,164] as well as XRD and TEM.[84] It was noted that Pt redispersion was accompanied by an increase in the Pt oxidation state; the oxidation of crystalline Pt and Pt redispersion were found to be conjoined processes. Because the "redispersing oxidation" occurred only in the presence of the chloride, it was concluded that mobile $Pt^{IV}O_xCl_y$ was responsible for the redispersion. This was reinforced by the temperature range in which redispersion occurred (500−600 °C), which corresponds to the temperature range where the $Pt^{IV}O_xCl_y$ complex can be formed.[161]

The effect of chlorine (in the form of HCl, Cl_2, or CCl_4) on the dispersion of Pt has been known for some time.[165] There are other reported studies on the effect of Cl_2 and HCl on the redispersion of Pt over a range or materials, including zeolites.[166] The oxychlorination consisted of heated treatments (at 450, 620, or 720 °C) under a flow of 400 ppm of CCl_4 in O_2, which were followed by reduction (500 °C for 16 h). The reported optimum temperature for the Pt dispersion was 620 °C. The results of the study with CCl_4 reinforced the previously reported view[163,164,166] that the creation of oxychloroplatinum or chloroplatinum species was the important step in the redispersion process.

Two sintered Pt/Al_2O_3 catalysts (0.6 and 1 wt % Pt) underwent successful Pt redispersion at 500 °C in an oxychlorination treatment with 2% O_2 in a $HCl/H_2O/N_2$ feed (H_2O to HCl molar ratio of 56) for up to 8 h.[167] The treated samples were analyzed using TPR, hydrogen chemisorption, TEM, and EXAFS. Chemisorption results indicated that the oxychlorination led to an increased Pt dispersion. TEM results (See Figure 2) indicated the presence of particles 15−20

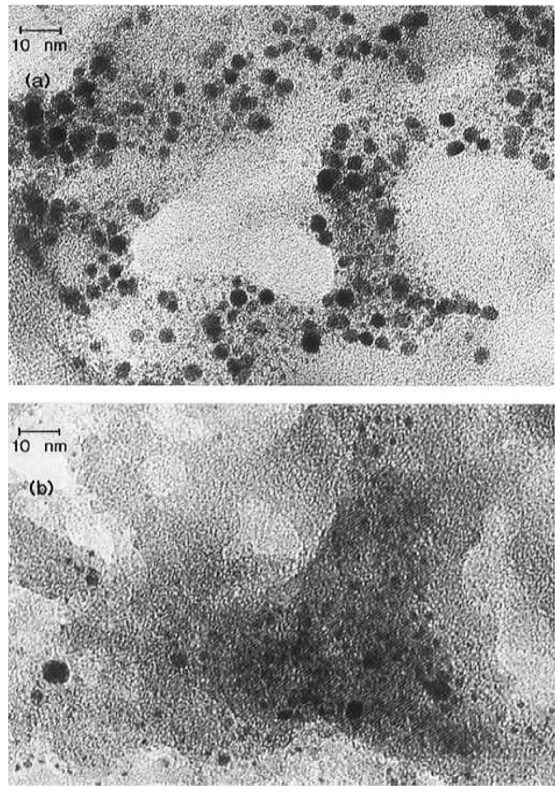

Figure 2. TEM micrographs of 0.6 wt % Pt/Al_2O_3; sintered (a) and redispersed (b).[167]

DOI: 10.1021/acscatal.5b00535
ACS Catal. 2015, 5, 3430−3445

nm in size in the sintered sample, compared with particles 6−8 nm in size over the redispersed catalyst. EXAFS results reported that the Pt−Pt coordination numbers also decreased as a result of the oxychlorination treatments. The EXAFS results also indicated the presence of some Pt−O and Pt−Cl coordination during the redispersion process, which would be indicative of the formation of some oxychloroplatinum species, most likely $[Pt_s(OH)_4Cl_2]^{2-}$.

In another study of a Pt/Al_2O_3 catalyst (which was also prechlorided with HCl during impregnation) that used HCl in the oxychlorination treatment, the effect of oxygen partial pressure (from 0 to 100%) and HCl concentration (from 0.0005 to 0.003 atm) on redispersion were assessed.[168] In this case, the sintered catalyst had a Pt dispersion of ∼12%. The most effective temperature range for redispersion by oxychlorination was found to be 480−500 °C. In the absence of oxygen, further sintering was observed, highlighting the importance of oxygen in the redispersion. Furthermore, as the partial pressure of oxygen was increased (at fixed HCl concentration), the rate of redispersion was also found to increase. Analogously, when the HCl concentration was increased (at fixed O_2 concentration), it was also found to increase the rate of redispersion as well as increase the final dispersion achieved. Subsequently, a kinetic model for the sintering and redispersion processes of Pt on Al_2O_3 was also developed.[168]

XANES has been utilized along with hydrogen chemisorption and *n*-heptane reforming activity screening to monitor the effect of oxychlorination/reduction cycles on Pt/Al_2O_3.[169] Oxychlorination in the chemisorption studies was conducted by injecting 1,2-dichloropropane at a rate of 30 μL h^{-1} in the first cycle and 15 μL h^{-1} for all subsequent cycles. Reduction at 500 °C followed after the oxychlorination. For the XANES studies, oxychlorination was conducted during a temperature ramp up to 550 °C (at 6.8 °C min^{-1}) and a subsequent dwell time of 30 min. Again, 1, 2-dichloropropane (1270 ppm in He; halved for the subsequent cycles) was used with 45 cm^3 min^{-1} of air delivering ∼1% Cl to the sample. The results indicated that the oxychlorination resulted in an increased dispersion of Pt. This increased dispersion had an insignificant impact on the selectivity during the *n*-heptane reforming reaction.

It is also noteworthy that there are cases of Pt redispersion being achieved using hydrofluorination with HF.[170] Activation with HF was studied because the fluorine−aluminum bond is much stronger than the chlorine−aluminum bond and, as such, was seen as an alternate to the need for constant injection of halohydrocarbon, as is typically the case with chloro compounds in industrial reactors.[19] Primarily, this treatment (doping 0.2 wt % Pt/H-ZSM-5 with up to 3% HF) increases both acid strength and the number of acidic sites, which increased selectivity for methylation of toluene to xylenes (and reducing side reaction to trimethylbenzenes) as a result of the changes in shape of the active site. However, it was also noted from H_2 pulse chemisorption that there was an apparent increase in the Pt dispersion when the catalysts were doped with HF. Unfortunately, no microscopy was reported.

2.2.2. Palladium. A monolithic Pd three-way catalyst was treated by chlorination using submergence in HCl solution to achieve regeneration.[171] Hydrogen chemisorption was used to determine the dispersion of Pd and particle diameter, and it was calculated that the Pd dispersion was increased following the HCl treatment while the particle size decreased from 7 to 3 nm. SEM studies determined that there was a large quantity of particles of size 50−100 nm present in the aged (sintered) catalyst. Using the HCl treatment, although there were still some particles ∼100 nm in size, the number of these was reduced by ∼60%. Electron dispersive X-ray (EDX) analysis reported that the Pd/Al ratio also increased following the HCl treatment, which is evidence that the reduction in the number of larger particles is not due to leeching of Pd. It is worth noting, though, that the HCl treatment did not recover the original dispersion of the fresh catalyst. However, despite the original dispersion not being regained, it is still claimed that such regeneration methods have real prospects for automotive catalyst recycling because there is still the potential to prolong the lifetime of the catalyst.

A further example of Pd redispersion has been reported using Cl_2 diluted in a feed of oxygen and helium for the oxychlorination treatment.[172] A $Pd/CeO_2-Al_2O_3$ catalyst was studied with XRD, XPS, TEM, TPR, and oxygen storage capacity (OSC) measurements before and after a range of oxychlorination treatments (with varying concentrations of Cl_2) in the 500−850 °C temperature range. The results have indicated that the oxychlorination followed by reduction was very effective for redispersion of Pd, with average particle sizes decreasing from 17 nm to ∼8 nm. It was further found that at oxychlorination temperatures above 500 °C, there was no further significant redispersion of Pd.

2.2.3. Other Metals and Bimetallic Catalyst Systems. In addition to oxychlorination of Pt/Al_2O_3, the previously discussed study[169] also assessed the same treatments for a $Pt-Re/Al_2O_3$ bimetallic catalyst, and an increased dispersion was also reported in this case. However, in the case of the bimetallic catalyst, there was also increased selectivity to the hydrogenolysis products for the n-heptane reforming reaction. X-ray adsorption near edge spectroscopy (XANES) studies found that there was no Pt−Re alloy formation in the calcined catalyst, but that alloy formed during the reduction. Oxychlorination was found to disrupt the alloy, resulting in highly dispersed monometallic particles. All subsequent reductions again resulted in alloy formation, although the physical (particle size) and chemical (active metal distribution) nature of the alloyed species was significantly different from that formed after the initial reduction. This was due to the mobilization of the oxidized species (during oxychlorination) and the presence of chlorine.[169] Similar studies in which particle size reportedly decreased from 70 nm to ∼20 nm have been reported elsewhere.[173]

The effect of oxychlorination (followed by reduction) treatment on Pt/Al_2O_3 and $Pt-Sn/Al_2O_3$ has also been studied.[22,80] A series of six consecutive oxychlorination (1 h at 550 °C; 31 μmol h^{-1} of 1, 2-dichloropropane in 60 mL min^{-1} of air) and reduction (1 h at 400 °C; H_2) cycles were then employed for an infrared (IR) study.[22] Alternatively, the samples were calcined in air during a 15 °C min^{-1} temperature ramp up to 400 °C (followed by a 30 min dwell), followed by reduction at 400 °C for 1 h in H_2. Then an oxidation (in air, at 550 °C for 1 h) was followed by a further reduction (in H_2, at 400 °C for 1 h). A series of consecutive oxychlorination (1 h at 550 °C; 510 μmol h^{-1} of 1, 2-dichloropropane per 50 mg of catalyst, in 60 mL min^{-1} of air) and reduction (1 h at 400 °C; H_2) cycles were then employed.[80]

It was noted that any sintering occurring during oxidation−reduction could be reversed by oxychlorination−reduction treatment. From the IR spectroscopy, it was reported that oxychlorination caused the formation of (oxy)chloroplatinum

DOI: 10.1021/acscatal.5b00535
ACS Catal. 2015, 5, 3430−3445

species on the surface. Hence, in the absence of chlorine, the Pt tended to sinter, and the redispersion in the oxychlorination can be attributed to the formation of these (oxy)-chloroplatinum species, which are mobile on the support surface and decompose during reduction to form small clusters of Pt atoms.[22]

For the oxychlorinated Pt−Sn/Al_2O_3 catalysts, the presence of Sn significantly reduced the formation of chloroplatinum and oxychloroplatinum complexes (by up to 50%). Excess Sn favored alloy formation in the presence of chlorine, hindering the migration of Pt through competition for support sites.[80] Hence, the reduced catalyst (after oxychlorination) also had a significantly lower dispersion than was observed in the absence of Sn.

Similar work on the oxychlorination treatments of Pt/Al_2O_3, Re/Al_2O_3, and Pt−Re/Al_2O_3 catalysts has been conducted using the same preparation conditions previously mentioned herein.[18,79] Instead of the oxidative treatment, however, the oxychlorination involved heating the samples to 550 °C and introducing 1,2-dichloropropane (60 μL h^{-1} per gram of catalyst) into the 60 mL min^{-1} feed of CO_2-free air for 1 h.[18,79] Similar studies, with similar results, have been reported elsewhere.[158]

In the case of the monometallic catalysts, the Pt dispersion was increased during the oxychlorination, but this was not the case for Re. The Pt dispersion of the bimetallic catalyst was also increased. The oxychlorination formed chloroplatinum and oxychloroplatinum complexes (in the case of the bimetallic these were free of Re), and this improved the Pt dispersion (after reduction) because the Pt complexes were able to migrate across the alumina. As before,[22,80] the oxychlorination has also been found to reverse the sintering and the existence of Pt−Re bimetallic particles that occurred following oxidation and reduction cycles.[18,79]

In combination with the oxidation and reduction cycles (as discussed in previous section), oxychlorination was also investigated for Pd/Rh monolith catalysts.[122] The addition of chlorine to the oxygen feed (0.8 Cl_2, 18% O_2, balance N_2) resulted in a marked improvement in the activity of the aged catalyst, and this has been attributed to an increased rate of dispersion of the metals on the surface.[174] The greater efficiency of the oxychlorination compared with the oxidation treatment is further reinforced by the fact that the oxy-chlorination was conducted for only 1 h, as opposed to 10 h for the chlorine-free treatment.

The use of 1,2-dichloropropane as a source of chlorine for oxychlorination treatments has been further applied to Pd−Rh catalysts supported on a mixed ceria−zirconia−alumina support, albeit with slightly different conditions (80 μL h^{-1} 1,2-dichloropropane in 50 mL min^{-1} of N_2).[175] As has been demonstrated already, the oxychlorinations were able to reverse the Pd sintering process of thermal treatments, resulting in higher Pd dispersions, along with the recovery of the oxygen storage capacity of the support through stronger metal−ceria zirconia interactions.

In the case of a Pt−Rh catalyst supported on a ceria zirconia alumina support,[176] the same recovery of oxygen storage capacity was not achieved, but this could be due to different strengths of the interaction between the metal and support.[175] A similar study has been reported for a Pt−Re/Al_2O_3, except that C_2HCl_3 was used as the source of chlorine.[177]

A structured monolith Pd−Rh three-way catalyst was also treated with chlorine reagents (1,2-dichloropropane and dichloroacetic acid) using 0.1 M solutions flowing at 0.6 L min^{-1} at 50 °C for 2 h,[178] a procedure that has been reported before for the regeneration of other monolith samples via removal of poisons.[179,180] The dichloroacetic acid was found to be more effective than dichloropropane at recovering Pd active sites, which has been attributed to the apparent redispersion and restructuring of said Pd due to the chlorination and subsequent reduction. This redispersion had the additional benefit of recovering oxygen storage capacity, as has been noted in a number of cases. It should be noted, however, that no microscopy has been utilized to establish any effectual change in metal particle size, so one cannot rule out that this recovery of Pd active sites is not redispersion at all, but rather, it is the removal of coke or other poisons.

The promotional effect of chlorine or fluorine on metal (Pt, Ir, Rh, Re, or U) or bimetallic (Pt−Ir, Pt−Rh, Pt−Re, or Pt−U) dispersion when supported on γ-Al_2O_3 catalysts has also been studied for a number of reactions. The pulsed microreactor experiments studied with these catalysts included hydro-genation of aromatics (benzene or toluene),[181] the dehydro-genation of cyclohexane,[182] and the hydroconversion of cyclohexene.[183] The catalysts were doped with halogen using ammonium chloride or ammonium fluoride, with an optimum halogen content found to be 3%. The dispersion of metallic/bimetallic particles was determined using a hydrogen pulse chemisorption technique. In most cases, the treatment with halogen resulted in an apparent higher dispersion of the metallic/bimetallic particles. No other techniques were utilized to determine particle sizes, and as such, the study is certainly not definitive in proving that the particle size had changed. In terms of promotion of the catalyst activity, it was reported that chloride was better than fluoride for the monometallic catalysts, whereas in the case of the bimetallic catalysts, chloride inhibited the activity while fluoride promoted activity. The proposed reason was that, in the case of monometallic catalysts, metal fluorides formed, which because of obvious electronegativity differences, form stronger bonds than analogous chloride species, making it more difficult to produce metallic particles in the case of the fluorides. For the bimetallic catalysts, however, clusters of metals are reportedly formed, which reduces the amount of metal−halide formation.

While studying cyclohexene hydroconversion, Pt−Re/H-ZSM-5 catalysts were investigated for activation by doping (3%) with HCl or HF.[19] Additionally, the monometallic Re catalyst was investigated in a similar manner. The metal dispersion was calculated using hydrogen pulse chemisorption, and doping with the halo acids was found to increase the apparent dispersion. In the case of the monometallic Re catalysts, the HF doping resulted in the best metal dispersion, whereas HCl gave the highest dispersion in the case of the bimetallic catalyst (although this was still less than that of the HF doped monometallic catalyst). Although XRD was used, the diffractograms were not published because it was reported that similar reflection intensities for all samples were observed. Consequently, no quantitative discussion in terms of changes in particle size was reported.

These typical oxychlorination treatments have been found not to be effective for some metals. For instance, although Pt does redisperse in a Pt−Ir/γ-Al_2O_3 catalyst, the Ir particle size was unchanged if the chloride content of the catalyst was too low.[184] However, by increasing the chloride content (e.g., up to 1.9 wt %) of the catalyst, oxychlorinations using low concentrations of chloride species (e.g., HCl) could generate

DOI: 10.1021/acscatal.5b00535
ACS Catal. 2015, 5, 3430−3445

chlorine in situ, a process that was also found to redisperse the Ir.[184] This may be due to weaker Ir metal−support interactions because in the case of Pt on SiO_2, in which the interaction is less than in the case of Pt−Al_2O_3, a higher concentration of chlorine (to form the complex) and a lower temperature (to stabilize the complex) was required.[185] However, in some cases, the complex formed may have a low volatility (e.g., $IrCl_3$) compared with the analogous Pt species and so may also require a higher temperature to induce vapor phase mobility,[174] a key aspect in redispersion. This aspect shows that the redispersion process sometimes has to be a trade-off in terms of temperatures because if the temperature is too high and the vapor phase chlorine complex too mobile, then leaching of the metal can occur (>700 °C in the case of Pt/Al_2O_3).[185]

2.2.4. Summary. A general mechanism for the redispersion by chlorination/oxychlorination has been proposed:[46,161,167]

- Surface atoms of metal crystallite oxidized by oxygen
- Oxidized sites are attacked by chloride ions, forming MO_xCl_y species
- The MO_xCl_y species fragment from the larger particle
- Mobile MO_xCl_y migrate to the support surface
- The metal is removed from the crystallite and redispersed

It should be noted that some reports mention the formation of halo metal complexes,[186] as opposed to oxyhalometal species. It is also important to note that chlorination may not work on some supports. For instance, chlorine could not prevent growth of Pt on a SiO_2 support.[159,187]

2.3. Thermal Treatment with Iodomethane. An issue arising from the use of the chlorination and oxychlorinations is the potential for further deactivation of the catalysts due to chlorine poisoning.[188] Consequently, other halogens potentially easier to remove from the catalyst post-treatment have been investigated. Iodomethane treatments have proven to be successful in the redispersion of metals to smaller nanoparticles, primarily in the case of gold,[188−190] but also for other metals (for example, rhodium).[191] A number of patents that use iodomethane as a promoter in an industrial process using a gold catalyst have previously been issued,[192,193] although no mention was made regarding an effect on the dispersion. The original treatment consisted of cofeeding iodomethane (or bromomethane[188]) in the reaction mixture for vapor phase methanol carbonylation over gold catalysts.[188−191] This resulted in structural transformation from gold particles of >10 nm to clusters of two or three gold atoms.[188−190] However, this treatment was originally performed under harsh conditions (240 °C and 16 bar)[189,192,193] which, although ideal for methanol carbonylation, would not necessarily be well suited for the wider application of redispersive treatments with iodomethane. Further investigation found that with treatments conducted with vapor phase iodomethane at atmospheric pressure and lower temperatures, redispersion of gold could still be achieved (atomic dispersion observed for temperature as low as 50 °C).[188] In an additional study using the same atmospheric conditions, similar results were also obtained for Au supported on metal oxides, including silica, titania, and alumina.[190]

In Figure 3, EXAFS data clearly shows that the as-received catalyst sample contained large Au particles, with the peak at 2.85 Å indicative of Au···Au coordination and the presence of other peaks at higher coordinations (5−6 Å). After 10 h of the methanol carbonylation reaction (which occurred at 16 bar

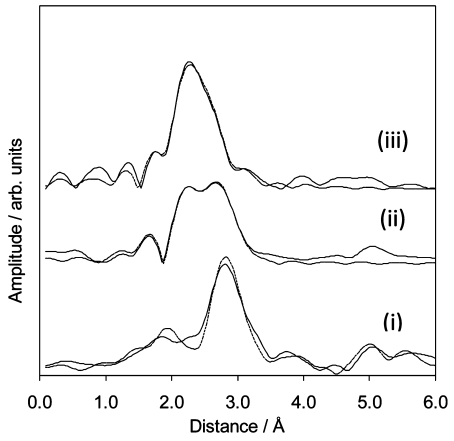

Figure 3. Comparison of experimental (solid) and fitted (dashed) EXAFS data of Au/C catalyst: as received (i) and after 10 (ii) and 80 h (iii) of methanol carbonylation reaction.[189]

pressure), the amplitude of the peaks at 2.85 Å and above began to decrease while a new peak at 2.5 Å began to emerge that was attributed to the restructuring and redispersion of gold particles. After 80 h of the methanol carbonylation reaction, this restructuring and redispersion has continued, as is evident from the complete disappearance of the peak at 2.85 Å and the continued decrease in amplitude of higher coordinations (between 5 and 6 Å), as well as the continued increase in the amplitude of the peak at 2.5 Å.

Similar observations were made whenever the iodomethane treatment was conducted at atmospheric pressure for 1 h, as is reported in Figure 4. Clearly the as-received Au/C catalyst in this case has some very large gold particles, as can be seen in parts A and B, the micrograph and particle size distribution of this sample, respectively. Importantly, parts C and D show that the iodomethane treatment is very effective at redispersion of

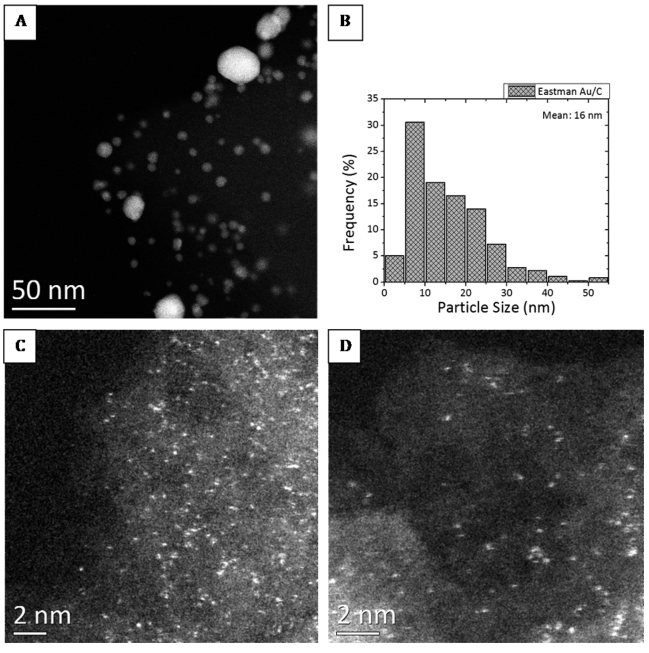

Figure 4. The influence of iodomethane on Au nanoparticles of Au/C. HAADF-STEM images of as received sample (a) and after iodomethane treatment at 240 °C for 1 h (c and d) as well as the particle size distribution of the as-received sample (b).[188]

DOI: 10.1021/acscatal.5b00535
ACS Catal. 2015, 5, 3430−3445

gold because, after only 1 h, it is apparent that the gold exists as isolated gold atoms, gold dimers, or subnanometer Au clusters. These findings were reinforced by the XRD results (Figure 5), where it is shown that the reflections of gold begin to decrease after only 1 min and, in fact, are no longer present after only 15 min of treatment with iodomethane.

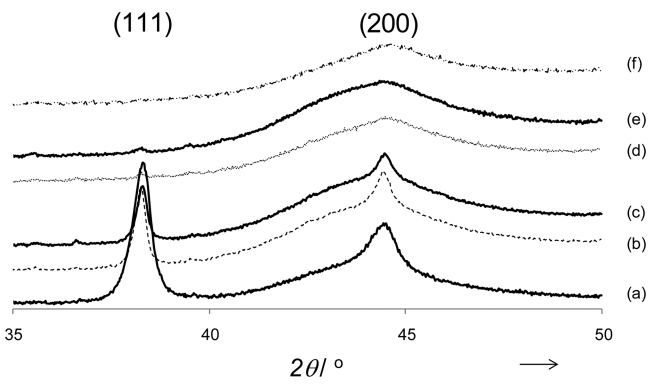

Figure 5. X-ray diffractograms of Au/C catalysts: as received (a) and after treatment with iodomethane for 1 (b), 5 (c), 15 (d), 30 (e), and 60 min (f).[188]

With such iodomethane treatments, there is an obvious need to remove any residual iodo species to prevent any adverse effect of halide on the catalyst. With this in mind, a reductive treatment at 190 °C was applied using 10% H_2 in Ar (20 cm^3 min^{-1}) and was found to be successful for the removal of residual iodo species without significantly affecting the dispersion of the gold particles.

The vapor phase iodomethane treatment has been studied for its potential to recover activity in a previously sintered catalyst, namely, Au supported on a ceria−zirconia−titania mixed oxide.[194] The iodomethane treatment produced an active catalyst (50% conversion at 175 °C) with a higher performance than the sintered catalyst (50% conversion at 375 °C). DRUV characterization of the sintered and treated catalysts indicated that the latter had some gold particles that are smaller in size than those found in the sintered sample.

2.3.1. Summary. A general mechanism for the redispersion by iodomethane can be proposed:

- Surface atoms of large gold clusters are attacked by iodide ions, forming Au_yI_z
- These Au_yI_z species become "etched" away from the surface of the cluster
- Mobile Au_yI_z migrates to the support surface
- A new layer of Au is exposed and attacked by iodide, and the process is repeated

2.4. Treatment with Alternative Halohydrocarbons. Due to the toxic and carcinogenic nature of iodomethane, a number of alternate halohydrocarbons were studied to develop safer vapor and liquid phase treatments.[9] Vapor phase treatments focused on the comparison of the original iodomethane treatment with *n*-iodobutane. These iodoalkanes were also used for liquid phase treatments, as were *p*-iodotoluene and the analogous bromo compounds. All of these alternative compounds have fewer risks associated with them and also happen to be less expensive than iodomethane.[9]

The catalyst used for this study was a 1 wt % Au/C, which had an average particle size of 27 nm and a dispersion of 3.3%. The same atmospheric conditions for the previously discussed vapor phase treatments using iodomethane were applied to the other iodoalkanes.

In the liquid phase treatments, the pure and hexane-diluted halohydrocarbon was mixed directly with the catalyst at 40 °C. Following these treatments, significant changes to the Au/C as a result of the treatments with halohydrocarbons were observed. In all cases, with the exception of the halotoluene samples, each halohydrocarbon had a varying ability to redisperse the gold to smaller nanoparticles. More specifically, the iodo based molecules were better at the dispersion than the analogous bromo based molecules, and the ability to redisperse gold increased with increasing alkane chain length. This was related to the strength of the alkyl−halide bond; that is, the weaker this bond strength, the greater the ability to redisperse the gold. This also explains the ineffectiveness of the halotoluenes, since the alkyl−halide bond strengths for these compounds are higher than those of the haloalkanes that were investigated. The reported results clearly demonstrated the possibility of using alternate haloalkanes to replace iodomethane for the redispersion of gold particles. Added to this, not only were some of these alternate halohydrocarbons less expensive, but some have been found to be just as efficient, if not better, at the redispersion of large gold particles.

Clearly, a successful alternate method of treatment has also been established through the use of liquid systems, which is obviously a less demanding process than the vapor phase treatment, which requires the catalyst to be heated to 240 °C. This alternative lower temperature liquid phase method of treatment was essentially as efficient as the vapor phase approach.

Additionally, a trend in the ability of redispersion of gold has been determined that is based on the bond strength of the R−X bond. It will now be possible to continue gold redispersion with alternative haloalkane compounds while reducing the risk of toxic contamination and carcinogenic exposure from iodomethane. A halide-free catalyst post-treatment was achieved using the same hydrothermal treatment previously employed for the original vapor phase iodomethane-treated samples.

2.4.1. Summary. The mechanism for this process is proposed to be the same as that which has been proposed for the iodomethane process in the previous section that involves formation of gold halide species on the surface of large gold particles, followed by the etching of these gold halide species. Hence, the general mechanism for the redispersion by halohydrocarbons can be proposed as

- Surface atoms of large gold clusters are attacked by haldide ions, forming Au_yX_z
- These Au_yX_z species become "etched" away from the surface of the cluster
- Mobile Au_yX_z migrate to the support surface
- A new layer of Au is exposed and attacked by halide, and the process is repeated

3. OVERVIEW

A number of mechanisms/modes of redispersion have been suggested, including molecular or atomic migration caused by changes in the wetting angle, SMSI/SMOI effects, surface erosion (resulting in heterogeneous particle sizes), or homogeneous splitting. It should be noted that the same trends are not always observed using identical conditions for catalysts comprised of the same constituents (i.e., model versus real catalysts).[195−197] It has been reported, though, that this can

DOI: 10.1021/acscatal.5b00535
ACS Catal. 2015, 5, 3430−3445

be simply down to differences in preparation of the catalysts.[195] This is also applicable to sintering because Pt−HY catalysts (prepared by ion exchange) are more likely to sinter than Pt/Al_2O_3 (prepared by impregnation).[40]

Predominantly, the mechanism of redispersion (sometimes referred to as the "strain model")[198] is similar in most cases. In terms of oxidation/reduction cycles, oxidation causes the large metallic agglomerates to undergo oxidation, forming oxymetal species on the surface of the particle. The variation in metal−metal distances in the metal oxide surface layer and those in the unoxidized metal induces a metal strain energy.[81] Consequently, the oxymetal particles progressively fragment from the large particle (by fracture of the larger particle)[78,81] and migrate and disperse due to interactions with the support,[196−198] then the newly exposed surface of the agglomerate is oxidized, and the process continues, resulting in highly dispersed oxymetal species throughout the catalyst. Under reducing conditions, these oxymetals revert to metallic form, but remain in a highly dispersed state. However, if reduction conditions are too harsh (e.g., temperature or treatment time), then sintering will occur again. Similar redispersion processes occur for halogen treatments (chlorination, oxychlorination, iodomethane, halohydrocarbons) but with the formation of intermediate halometal or oxyhalometal species (as opposed to oxymetal species).

In all cases, the smaller halometal/oxyhalometal particles undergo transport in the vapor phase through the support and subsequent reduction treatments, then result in highly dispersed metal particles. There is, however, a difference between chlorinations/oxychlorinations and iodomethane/halohydrocarbons in the process of the removal of halometal/oxyhalometal species from the large particles (see Figure 6). For chlorinations/oxychlorinations, the larger cluster of halometal/oxyhalometal species fragments/splits (process 1, Figure 6).

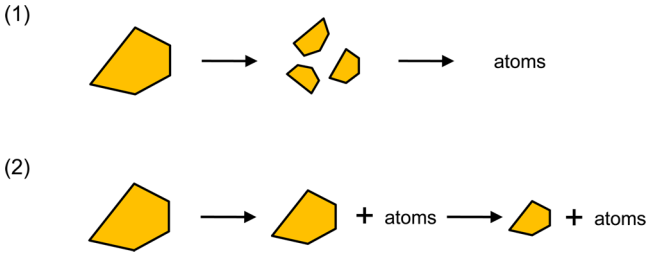

Figure 6. Processes of particle erosion.

In the case of the iodomethane and the other halohydrocarbons, redispersion occurs rapidly as the large particles' diameters shrink and erode as a result of the progressive removal of Au−X entities from the surface of the main particles (process 2, Figure 6).

In terms of applicability of the different redispersion methods and which of these might be best, it is fair to say that there is not a one-size-fits-all approach. As was indicated previously in this Perspective, the strength of the interactions between the metal and the support are specific to both the metal and the support. Since all the redispersion methods are an extension of metal/support interactions, the best method for redispersion of metals will also be specific to both the metal and the support. For instance, it is known that oxychlorinations are not suitable for gold because of chlorine poisoning or gold leaching. Although poisoning with the iodine can occur, it has also been demonstrated that the residual iodine can be removed with relatively mild treatments. The applicability of the iodo-based treatments to other metals is as yet unknown because there are no reported incidences that this has been investigated for any metal other than gold.

4. PERSPECTIVE

The prospects of using redispersion treatments to regenerate catalysts have been summarized above, and it clear that it is possible to regain or improve upon the original dispersion of catalysts that have been sintered. Although some of the reported redispersion processes have been conducted ex situ, there is great potential that any of these treatments could be used within existing processes. For instance, in a system of parallel reactors with a switchable feed, one reactor could be utilized for reaction while the catalyst is regenerated by redispersion in the coupled reactor. By doing so, catalyst lifetime could be increased by maintaining catalyst activity for a longer period of time. The additional benefit, in particular from the halohydrocarbon treatments, of the ability to tune the size of the metal nanoparticles has the potential to improve upon activity and selectivity.[9] As such, the ability of halohydrocarbons to redisperse metals other than gold is worthy of further investigation.

AUTHOR INFORMATION

Corresponding Authors

*E-mail: kmorgan08@qub.ac.uk.
*E-mail: c.hardacre@qub.ac.uk.

Notes

A number of figures in this Perspective have been reproduced, and the original work has been cited accordingly. Figure 1 is reprinted with permission from Kartusch et al., J. A. *ACS Catal.* **2012**, 2, 1394−1403; copyright 2012 American Chemical Society. Figure 2 is reprinted with permission from Le Normand et al. *J. Phys. Chem.* **1996**, 100, 9068−9076; copyright 1996 American Chemical Society. Figure 3 is reprinted with permission from Goguet et al. *J. Am. Chem. Soc.* **2009**, 131, 6973−6975; copyright 2009 American Chemical Society. Figures 4 and 5 are reprinted with permission from Sá et al. *Chem. Int. Ed.* **2011**, 50, 8912−8916; copyright 2011 Wiley-VCH Verlag GmbH & Co. KGaA, Weinheim.
The authors declare no competing financial interests.

ACKNOWLEDGMENTS

We gratefully acknowledge financial support from King Abdulaziz University (Grant No. D-005/431), and the CASTech Grant (EP/G012156/1) from the EPSRC.

REFERENCES

(1) Forzatti, P.; Lietti, L. *Catal. Today* **1999**, *52*, 165−181.
(2) Jackson, S. D. *Chem. Eng. J.* **2006**, *120*, 119−125.
(3) Sie, S. T. *Appl. Catal., A* **2001**, *212*, 129−151.
(4) Rodriguez, J. A.; Hanson, J. C.; Chupas, P. J. Introduction: Goals and Challenges for the in-situ Characterization of Heterogeneous Catalysts. In *In-situ Characterization of Heterogeneous Catalysts*; Rodriguez, J. A., Hanson, J. C., Chupas, P. J., Eds.; John Wiley and Sons: Hoboken, New Jersey, USA, 2013; pp 1−22.
(5) Jacques, S. D. M.; Di Michiel, M.; Kimber, S. A. J.; Yang, X.; Cernik, R. J.; Beale, A. M.; Billinge, S. J. L. *Nat. Commun.* **2014**, *4*, 2536.

DOI: 10.1021/acscatal.5b00535
ACS Catal. 2015, 5, 3430−3445

(6) Hanson, J. C.; Si, R.; Xu, W.; Senanayake, S. D.; Mudiyanselage, K.; Stacchiola, D.; Rodriguez, J. A.; Zhao, H.; Beyer, K. A.; Jennings, G.; Chapman, K. W.; Chupas, P. J.; Martinez-Arias, A. *Catal. Today* **2014**, *229*, 64−71.
(7) Yang, B.; Lin, X.; Nilius, N.; Freund, H.-J.; Hulot, C.; Giraud, A.; Blechert, S.; Tosoni, S.; Sauer, J. *J. Am. Chem. Soc.* **2012**, *134*, 11161−11167.
(8) Behafarid, F.; Rodan Cuenya, B. *Top. Catal.* **2013**, *56*, 1542−1559.
(9) Morgan, K.; Burch, R.; Daous, M.; Delgado, J. J.; Goguet, A.; Hardacre, C.; Petrov, L. A.; Rooney, D. W. *Catal. Sci. Technol.* **2014**, *4*, 729−737.
(10) Romero-Sarria, F.; Martinez T, L. M.; Centeno, M. A.; Odriozola, J. A. *J. Phys. Chem. C* **2007**, *111*, 14469−14475.
(11) Haruta, M. *Catal. Today* **1997**, *36*, 153−166.
(12) Boccuzzi, F.; Manzoli, M.; Chiorino, A.; Vindigni, F. Insights into the Reactivity of Gold: An Analysis of FTIR and HRTEM Studies. In *Environmental Catalysis over Gold-Based Materials*; Avgouropoulos, G., Tabakova, T., Eds.; RSC Catalysis Series; The Royal Society of Chemistry: Cambridge, UK, 2013; pp 63−95.
(13) Heck, R. M.; Farrauto, R. J.; Gulati, S. T. Catalyst Deactivation. *Catalytic Air Pollution Control: Commercial Technology*; John Wiley and Sons: Hoboken, New Jersey, USA, 2002; pp 63−73.
(14) Fang, Z. Z.; Wang, H. Sintering of Ultrafine and Nanosized Particles. In *Sintering of Advanced Materials*; Fang, Z. Z., Ed.; Woodhead Publishing Limited: Cambridge, UK, 2010; pp 434−474.
(15) Campbell, C. T. *Acc. Chem. Res.* **2013**, *46*, 1712−1719.
(16) Susu, A. A.; Ogogo, E. O.; Ngomo, H. M. *Trans. IChemE Part A Chem. Eng. Research & Design* **2006**, *84*, 664−676.
(17) Banerjee, A.; Theron, R.; Scott, R. W. J. *Chem. Commun.* **2013**, *49*, 3227−3229.
(18) Chong, F. K.; Anderson, J. A.; Rochester, C. H. *Phys. Chem. Chem. Phys.* **2000**, *2*, 5730−5736.
(19) Kluksdahl, H. E. US Patent 3,415,737, 1968.
(20) Aboul-Fotouh, S. M. K.; Aboul-Gheit, N. A. K. *Chin. J. Catal.* **2012**, *33*, 697−705.
(21) Fung, A. S.; Kelley, M. J.; Koningsberger, D. C.; Gates, B. C. *J. Am. Chem. Soc.* **1997**, *119*, 5877−5887.
(22) Arteaga, G. J.; Anderson, J. A.; Rochester, C. H. *J. Catal.* **1999**, *184*, 268−279.
(23) Bacaud, R.; Bussiere, P.; Figueas, F. *J. Catal.* **1981**, *69*, 399−409.
(24) McVicker, G. B.; Garten, R. L.; Baker, R. T. K. *J. Catal.* **1978**, *54*, 129−142.
(25) Arnal, P. M.; Comotti, M.; Schuth, F. *Angew. Chem., Int. Ed.* **2006**, *45*, 8224−8227.
(26) Botella, P.; Corma, A.; Navarro, M. T.; Quesada, M. *J. Mater. Chem.* **2009**, *19*, 3168−3175.
(27) Somorjai, G. A.; Park, J. Y. *Top. Catal.* **2008**, *49*, 126−135.
(28) Joo, S. H.; Park, J. Y.; Tsung, C.-K.; Yamada, Y.; Yang, P.; Somorjai, G. A. *Nat. Mater.* **2009**, *8*, 126−131.
(29) Yin, Y. D.; Rioux, R. M.; Erdonmez, C. K.; Hughes, S.; Somorjai, G. A.; Alivisatos, A. P. *Science* **2004**, *304*, 711−714.
(30) Wang, X.; Rodriguez, J. A.; Hanson, J. C.; Gamarra, D.; Martinez-Arias, A.; Fernandez-Garcia, M. *J. Phys. Chem. B* **2005**, *109*, 19595−19603.
(31) Hatanaka, M.; Takahashi, N.; Takahashi, N.; Tanabe, T.; Nagai, Y.; Suda, A.; Shinjoh, H. *J. Catal.* **2009**, *266*, 182−190.
(32) Ciston, J.; Si, R.; Rodriguez, J. A.; Hanson, J. C.; Martinez-Arias, A.; Fernandez-Garcia, M.; Zhu, Y. *J. Phys. Chem. C* **2011**, *115*, 13851−13859.
(33) Kurnatowska, M.; Kepinski, L.; Mista, W. *Appl. Catal., B* **2012**, *117*−*118*, 135−147.
(34) Farmer, J. A.; Campbell, C. T. *Science* **2010**, *329*, 933−936.
(35) Aydin, C.; Lu, J.; Browning, N. D.; Gates, B. C. *Angew. Chem., Int. Ed.* **2012**, *51*, 5929−5934.
(36) Fiedorow, R. M. J.; Chahar, B. S.; Wanke, S. E. *J. Catal.* **1978**, *51*, 193−202.
(37) Hernandez, W. Y.; Romero-Sarria, F.; Centeno, M. A.; Odriozola, J. A. *J. Phys. Chem. C* **2010**, *114*, 10857−10865.
(38) Bruix, A.; Rodriguez, J. A.; Ramirez, P. J.; Senanayake, S. D.; Evans, J.; Park, J. B.; Stacchiola, D.; Liu, P.; Hrbek, J.; Illas, F. *J. Am. Chem. Soc.* **2012**, *134*, 8968−8974.
(39) Tripković, V.; Cerri, I.; Nagami, T.; Bligaard, T.; Rossmeisl, J. *Phys. Chem. Chem. Phys.* **2013**, *15*, 3279−3285.
(40) Weller, S. W.; Montagna, A. A. *J. Catal.* **1971**, *20*, 394−407.
(41) Adamiec, J.; Fiedorow, R. M. J.; Wanke, S. E. *J. Catal.* **1985**, *95*, 492−500.
(42) Tanaka, H.; Taniguchi, M.; Kajita, N.; Uenishi, M.; Tan, I.; Sato, N.; Narita, K.; Kimura, M. *Top. Catal.* **2004**, *30/31*, 389−396.
(43) Hageluken, C. *Platinum Met. Rev.* **2012**, *56*, 29−35.
(44) D'Aniello, M. J., Jr; Monroe, D. R.; Carr, C. J.; Krueger, M. H. *J. Catal.* **1988**, *109*, 407−422.
(45) Newton, M. A. *Chem. Soc. Rev.* **2008**, *37*, 2644−2657.
(46) Borgna, A.; Le Normand, F.; Garetto, T. F.; Apesteguia, C. R.; Moraweck, B. *Stud. Surf. Sci. Catal.* **1999**, *126*, 179−186.
(47) Flynn, P. C.; Wanke, S. E. *J. Catal.* **1974**, *34*, 390−399.
(48) Flynn, P. C.; Wanke, S. E. *J. Catal.* **1975**, *37*, 432−448.
(49) Rice, R. W.; Chien, C. C. *J. Catal.* **1987**, *103*, 140−150.
(50) Yao, H. C.; Sieg, M.; Plummer, H. K., Jr. *J. Catal.* **1979**, *59*, 365−374.
(51) Ruckenstein, E. *Metal-Support Interactions in Catalysis, Sintering and Redispersion*; Stevenson, S. A., Dumesic, J. A., Baker, R. T. K., Ruckenstein, E., Eds.; Van Nostrand Reinhold Catalysis Series; Van Nostrand: New York, USA, 1987; pp 141−308.
(52) Weiland, J. N. US Patent 2,330,462, 1943.
(53) Mekler, L. A. US Patent 2,391,327, 1945.
(54) Campbell O. F.; Decker, W. H. US Patent 2,853,455, 1958.
(55) Schwarzenbek, E. F. US Patent 3,230,179, 1966.
(56) Schutt, H. U. US Patent 3,558,514, 1971.
(57) McArthur, D. P. US Patent 4,039,471, 1977.
(58) Porcelli, R. V.; Bhise, V. S.; Shapiro, A. J. US Patent 4,252,741, 1978.
(59) Dawes, J. L.; Devon, T. J. US Patent 4,196,096, 1980.
(60) Chester, A. W. US Patent 4,235,754, 1980.
(61) Fung, S. C. US Patent 4,467,045, 1984.
(62) Upchurch, B. T.; Miller, I. M.; Brown, K. G.; Hess, R. V.; Schryer, D. R.; Sidney, B. D.; Wood, G. M., Paulin, P. A. US Patent 4,829,035, 1989.
(63) Harandi, M. N. US Patent 4,853,103, 1989.
(64) McKay, D. L.; Olbrich, M. E. US Patent 4,902,849, 1990.
(65) Feldman, R. J.; Dufallo, J. M.; Schwartz, W. A.; Williams, T. S. US Patent 5,315,056, 1994.
(66) Hagemeyer, A.; Watzenberger, O.; Deimling, O. US Patent 5,691,262, 1997.
(67) Brunet, F.-X.; Bromet, E.; Deves, J.-M. Humeau, D.; Snachez, E. US Patent 6,239,055, 2001.
(68) Capelle, M.; Deves, J.-M.; Hoffmann, F.; Thery, M. US Patent 6,426,052, 2002.
(69) Lew, L. E. US Patent 8,372,770, 2013.
(70) Sadasivan Vijaykumari, S.; Chewter, L. A.; van Westrenen, J. International Patent 2013079500, 2013.
(71) Lew, L. E. US Patent 8,815,201, 2014.
(72) Glassl, H.; Kramer, R.; Hayek, K. *J. Catal.* **1981**, *68*, 388−396.
(73) Tatarchuk, B. J.; Dumesic, J. A. *J. Catal.* **1981**, *70*, 308−322.
(74) Tatarchuk, B. J.; Dumesic, J. A. *J. Catal.* **1981**, *70*, 323−334.
(75) Tatarchuk, B. J.; Dumesic, J. A. *J. Catal.* **1981**, *70*, 335−346.
(76) Adler, S. F.; Keavney, J. J. *J. Phys. Chem.* **1960**, *64*, 208−212.
(77) Dautzenberg, F. M.; Wolters, H. B. M. *J. Catal.* **1978**, *51*, 26−39.
(78) Ruckenstein, E.; Chu, Y. F. *J. Catal.* **1979**, *59*, 109−122.
(79) Chong, F. K.; Anderson, J. A.; Rochester, C. H. *J. Catal.* **2000**, *190*, 327−337.
(80) Arteaga, G. J.; Anderson, J. A.; Becker, S. M.; Rochester, C. H. *J. Mol. Catal. A: Chem.* **1999**, *145*, 183−201.
(81) Ruckenstein, E.; Malhorta, M. L. *J. Catal.* **1976**, *41*, 303−311.
(82) Fiedorow, R. M. J.; Wanke, S. E. *J. Catal.* **1976**, *43*, 34−42.
(83) Jaworska-Galas, Z.; Wrzyszcz, J. *Int. Chem. Eng.* **1966**, *6*, 604−608.

DOI: 10.1021/acscatal.5b00535
ACS Catal. 2015, 5, 3430−3445

(84) Adamiec, J.; Szymura, J. A.; Wanke, S. E. *Stud. Surf. Sci. Catal.* **1993**, *75*, 1405−1418.
(85) Susu, A. A.; Ogogo, E. O. *J. Chem. Technol. Biotechnol.* **2006**, *81*, 694−705.
(86) Tanabe, T.; Nagai, Y.; Dohmae, K.; Sobukawa, H.; Shinjoh, H. *J. Catal.* **2008**, *257*, 117−124.
(87) Nagai, Y.; Hirabayashi, T.; Dohmae, K.; Takagi, N.; Minami, T.; Shinjoh, H.; Matsumoto, S. *J. Catal.* **2006**, *242*, 103−109.
(88) Nagai, Y.; Dohmae, K.; Ikeda, Y.; Takgai, N.; Tanabe, T.; Hara, N.; Guilera, G.; Pascarelli, S.; Netwon, M. A.; Kuno, O.; Jiang, H.; Shinjoh, H.; Matsumoto, S. *Angew. Chem.* **2008**, *120*, 9443−9446.
(89) Stulga, J. E.; Wynbatt, P.; Tien, J. K. *J. Catal.* **1980**, *62*, 59−69.
(90) Manga, N. H.; Susu, A. A. *Chem. Eng. Technol.* **1996**, *19*, 263−271.
(91) Johnson, M. F. L.; Keith, C. D. *J. Phys. Chem.* **1963**, *67*, 200−201.
(92) Hassan, S. A.; Khalil, F. M.; El-Gahal, F. G. *J. Catal.* **1976**, *44*, 5−14.
(93) Baker, R. T. K.; Prestridge, E. B.; Garten, R. L. *J. Catal.* **1979**, *59*, 293−302.
(94) Kubacka, A.; Martinez-Arias, A.; Fernandes-Garcia, M.; Di Michel, M.; Newton, M. A. *J. Catal.* **2010**, *270*, 275−284.
(95) Newton, M. A.; Di Michiel, M.; Kubacka, A.; Fernandez-Garcia, M. *J. Am. Chem. Soc.* **2010**, *132*, 4540−4541.
(96) Kubacka, A.; Iglesias-Juez, A.; Di Michiel, M.; Newton, M. A.; Fernandez-Garcia, M. *Phys. Chem. Chem. Phys.* **2013**, *15*, 8640−8647.
(97) Newton, M. A.; Belver-Coldeira, C.; Matinez-Arias, A.; Fernandez-Garcia, M. *Nat. Mater.* **2007**, *6*, 528−532.
(98) Newton, M. A.; Belver-Coldeira, C.; Matinez-Arias, A.; Fernandez-Garcia, M. *Angew. Chem.* **2007**, *119*, 8783−8785.
(99) Newton, M. A.; Belver-Coldeira, C.; Matinez-Arias, A.; Fernandez-Garcia, M. *Angew. Chem., Int. Ed.* **2007**, *46*, 8629−8631.
(100) Nishihata, Y.; Mizuki, J.; Akao, T.; Tanaka, H.; Uenishi, M.; Kimura, M.; Okamoto, T.; Hamada, N. *Nature* **2002**, *418*, 164−167.
(101) Tanaka, H.; Taniguchi, M.; Uenishi, M.; Kajita, N.; Tan, I.; Nishihate, Y.; Mizuki, J.; Narita, K.; Kimura, M.; Kaneko, K. *Angew. Chem., Int. Ed.* **2006**, *45*, 5998−6002.
(102) Smith, M. D.; Stepan, A. F.; Ramarao, C.; Brennan, P. E.; Ley, S. V. *Chem. Commun.* **2003**, 2652−2653.
(103) Andrews, S. P.; Stepan, A. F.; Tanaka, H.; Ley, S. V.; Smith, M. D. *Adv. Synth. Catal.* **2005**, *347*, 647−654.
(104) Ito, S.; Ishiguro, S.; Kunimori, K. *Catal. Today* **1998**, *44*, 145−149.
(105) Bernal, S.; Calvino, J. J.; Cauqui, M. A.; Perez Omil, J. A.; Pintado, J. M.; Rodriguez-Izquierdo, J. M. *Appl. Catal., B* **1998**, *16*, 127−138.
(106) Bernal, S.; Blanco, G.; Calvino, J. J.; Cifredo, G. A.; Gatica, J. M.; Perez Omil, J. A.; Pintado, J. M. *Stud. Surf. Sci. Catal.* **1994**, *82*, 507−514.
(107) Bernal, S.; Botana, F. J.; Calvino, J. J.; Cifredo, G. A.; Perez Omil, J. A.; Pintado, J. M. *Catal. Today* **1995**, *23*, 219−250.
(108) Yao, H. C.; Shelef, M. *J. Catal.* **1976**, *44*, 392−403.
(109) Olsthoorn, A. A.; Boelhouwer, C. *J. Catal.* **1976**, *44*, 197−206.
(110) Okal, J.; Kubicka, H.; Kępiński, L.; Krajczyk, L. *Appl. Catal., A* **1997**, *162*, 161−169.
(111) Okal, J.; Kubicka, H. *Appl. Catal., A* **1998**, *171*, 351−359.
(112) Okal, J.; Kepiński, L.; Krajczyk, L.; Drozd, M. *J. Catal.* **1999**, *188*, 140−153.
(113) Lai, X.; St.Clair, T. P.; Goodman, D. W. *Faraday Discuss.* **1999**, *114*, 279−284.
(114) Inceesungvorn, B.; Lopez-Castro, J.; Calvino, J.; Bernal, S.; Meunier, F. C.; Hardacre, C.; Griffin, K.; Delgado, J. J. *Appl. Catal., A* **2011**, *391*, 187−193.
(115) Breen, J. P.; Burch, R.; Hardacre, C.; Hill, C. J. *J. Phys. Chem. B* **2005**, *109*, 4805−4807.
(116) Shibata, J.; Shimizu, K. I.; Satokawa, S.; Satsuma, A.; Hattori, T. *Phys. Chem. Chem. Phys.* **2003**, *5*, 2154−2160.
(117) Goguet, A.; Hardacre, C.; Inceesungvorn, B.; Morgan, K.; Shekhtman, S. O. *Catal. Sci. Technol.* **2011**, *1*, 760−767.
(118) Breen, J. P.; Burch, R.; Hardacre, C.; Hill, C. J.; Krutzsch, B.; Bandl-Konrad, B.; Jobson, E.; Cider, L.; Blakeman, P. G.; Peace, L. J.; Twigg, M. V.; Preis, M.; Gottschling, M. *Appl. Catal., B* **2007**, *70*, 36−44.
(119) Nakatsuji, T.; Yasukawa, R.; Tabata, K.; Ueda, K.; Niwa, M. *Appl. Catal., B* **1998**, *17*, 333−345.
(120) Kartusch, C.; Krumeich, F.; Safanova, O.; Hartfelder, U.; Makosch, M.; Sa, J.; van Bokhoven, J. A. *ACS Catal.* **2012**, *2*, 1394−1403.
(121) Takasaki, S.; Takahashi, K.; Suzuji, H.; Sato, Y.; Ueno, A.; Kotera, Y. *Chem. Lett.* **1983**, 265−268.
(122) Birgersson, H.; Boutonnet, M.; Jaras, S.; Eriksson, L. *Top. Catal.* **2004**, *30/31*, 433−437.
(123) Kwak, J. H.; Dagle, R.; Tustin, G. C.; Zoeller, J. R.; Allard, L. F.; Wang, Y. *J. Phys. Chem. Lett.* **2014**, *5*, 566−572.
(124) Wang, T.; Schmidt, L. D. *J. Catal.* **1981**, *70*, 187−197.
(125) Lee, T. J.; Kim, Y. G. *J. Catal.* **1984**, *90*, 279−291.
(126) Kearby, K. K.; Thorn, J. P.; Hinlicky, J. A. US Patent 3,134,732, 1964.
(127) Kimberlin, C. N.; Gladrow, E. M. US Patent 3,201,355, 1965.
(128) Brown, H. T. US Patent 3,407,135, 1968.
(129) Glaser, H.; Sennewald, K.; Vogt, W. US Patent 2,488,295, 1966.
(130) Greenwood, A. R.; Vesley, K. D. US Patent 3,652,231, 1972.
(131) Kluksdahl, H. E. US Patent 3,764,557, 1973.
(132) Schott, S.; Lum, D. W.; Mador, I. L. US Patent 3,879,311, 1975.
(133) Yates, D. J. C.; Kmak, W. S. US Patent 3,937,660, 1976.
(134) Paynter, J. D.; Cecil, R. R. US Patent 3,939,061, 1976.
(135) Kmak, W. S.; Yates, D. J. C. US Patent 3,941,682, 1976.
(136) Paynter, J. D. US Patent 3,941,716, 1976.
(137) Kmak, W. S.; Yates, D. J. C. US Patent 3,943,052, 1976.
(138) Liederman, D.; Voltz, S. E. US Patent 3,950,491, 1976.
(139) Crowson, R.; Hargrove, J. D.; Pout, C. R. US Patent 3,986,982, 1976.
(140) Tauster, S. J.; Montagna, A. A.; Steger, J. J.; Fung, S. C.; Cross, V. R. US Patent 4,634,517, 1987.
(141) Borghard, W. S.; Huang, T. J.; McCullen, S. B.; Schoennagel, H. J.; Tsao, Y.-Y. P.; Wong, S. US Patent 4,657,874 1987.
(142) Hucul, D. A. US Patent 4,891,346, 1990.
(143) Cross, V. R.; Kao, J. L.; Vanderspurt, T. H.; Nadler, M.; Wortel, T. M. US Patent 4,914,068, 1990.
(144) Fung, S. C.; Tauster, S. J., Koo, J. Y. US Patent 4,925,819, 1990.
(145) Tsao, Y.-Y. P.; von Ballmoos, R. US Patent 4,929,576, 1990.
(146) Kellner, C. S. US Patent 5,057,470, 1991.
(147) Williamson, R. R.; Fettis, M. E.; Cottrell, P. R. US Patent 5,457,077, 1995.
(148) Huang, Y.-J. R.; Fung, S. C. US Patent 5,712,214, 1998.
(149) Fung, S. C.; Tauster, S. J.; Koo, J. Y. US Patent 5,763,348, 1998.
(150) Fung, S. C.; Tauster, S. J.; Koo, J. Y. US Patent 5,726,112, 1998.
(151) Capelle, M.; Deves, J.-M.; Hoffmann, F.; Thery, M. US Patent 6,133,183, 2000.
(152) Cottrell, P. R.; Fettis, M. E. European Patent 0,553,520, 1993.
(153) Capelle, M.; Deves, J.-M.; Hoffmann, F.; Thery, M. European Patent 0,872,276, 1998.
(154) Wu, A.-H. US Patent 8,664,144, 2014.
(155) Decoodt, X.; Durand, S.; Le-Goff, P.-Y.; Wermester, S. US Patent 8,673,801, 2014.
(156) Decoodt, X.; Durand, S.; Le-Goff, P.-Y.; Wermester, S. US Patent 8,680,000, 2014.
(157) Wu, A.-H. US Patent 8,716,161, 2014.
(158) Pieck, C.; Jablonski, E. L.; Parera, J. M. *Appl. Catal.* **1990**, *62*, 47−60.
(159) Baker, R. T. K.; Thomas, C.; Thomas, R. B. *J. Catal.* **1975**, *38*, 510−513.

DOI: 10.1021/acscatal.5b00535
ACS Catal. 2015, 5, 3430−3445

(160) Barbier, J.; Bahloul, D.; Marecot, P. *J. Catal.* **1992**, *137*, 377−384.
(161) Lieske, H.; Lietz, G.; Spindler, H.; Volter, J. *J. Catal.* **1983**, *81*, 8−16.
(162) Lietz, G.; Lieske, H.; Spindler, H.; Hanke, W.; Volter, J. *J. Catal.* **1983**, *81*, 17−25.
(163) Anderson, J. A.; Mordente, M. G. V.; Rochester, C. H. *J. Chem. Soc., Faraday Trans. 1* **1989**, *85*, 2983−2990.
(164) Anderson, J. A.; Mordente, M. G. V.; Rochester, C. H. *J. Chem. Soc., Faraday Trans. 1* **1989**, *85*, 2991−2998.
(165) Mordente, M. G. V.; Rochester, C. H. *J. Chem. Soc., Faraday Trans. 1* **1989**, *85*, 3495−3504.
(166) Foger, K.; Jaeger, H. *Appl. Catal.* **1989**, *56*, 137−147.
(167) Le Normand, F.; Borgna, A.; Garetto, T. F.; Apestegula, C.R.; Moraweck, B. *J. Phys. Chem.* **1996**, *100*, 9068−9076.
(168) Monzon, A.; Garetto, T. F.; Borgna, A. *Appl. Catal., A* **2003**, *248*, 279−289.
(169) Fernandez-Garcia, M.; Chong, F. K.; Anderson, J. A.; Rochester, C. H.; Haller, G. L. *J. Catal.* **1999**, *182*, 199−207.
(170) Aboul-Gheit, A. K.; Aboul-Enein, A. A.; Awadallah, A. E.; Ghoneim, S. A.; Emam, E. A. *Chin. J. Catal.* **2010**, *31*, 1209−1216.
(171) Birgersson, H.; Boutonnet, M.; Klingstedt, F.; Murzin, D. Y.; Stefanov, P.; Naydenov, A. *Appl. Catal., B* **2006**, *65*, 93−100.
(172) Lambrou, P. S.; Polychronopoulou, K.; Petallidou, K. C.; Efstathiou, A. M. *Appl. Catal., B* **2012**, *111−112*, 349−359.
(173) Cabello Galisteo, F.; Mariscal, R.; Lopez Granados, M.; Fierro, J. L. G.; Daley, R. A.; Anderson, J. A. *Appl. Catal., B* **2005**, *59*, 227−233.
(174) Foger, K.; Hay, D.; Jaeger, H. *J. Catal.* **1985**, *96*, 154−169.
(175) Daley, R. A.; Christou, S. Y.; Efstathiou, A. M.; Anderson, J. A. *Appl. Catal., B* **2005**, *60*, 117−127.
(176) Anderson, J. A.; Daley, R. A.; Christou, S. Y.; Efstathiou, A. M. *Appl. Catal., B* **2006**, *64*, 189−200.
(177) Pieck, C. L.; Vera, C. R.; Parera, J. M. *Study of industrial and laboratory regeneration of Pt-Re/Al_2O_3 catalysts*; 9th International Symposium on Catalyst Deactivation, Lexington, KY, October, 2001.
(178) Christou, S. Y.; Efstathiou, A. M. *Top. Catal.* **2013**, *56*, 255−260.
(179) Christou, S. Y.; Birgersson, H.; Fierro, J. L. G.; Efstathiou, A. M. *Environ. Sci. Technol.* **2006**, *40*, 2030−2036.
(180) Christou, S. Y.; Birgerssin, H.; Efstathiou, A. M. *Appl. Catal., B* **2007**, *71*, 185−198.
(181) Ali, A.-G. A.; Ali, L. I.; Aboul-Fotouh, S. M.; Aboul-Gheit, A. K. *Appl. Catal., A* **1998**, *170*, 285−296.
(182) Ali, L. I.; Ali, A.-G. A.; Aboul-Fotouh, S. M.; Aboul-Gheit, A. K. *Appl. Catal., A* **1999**, *177*, 99−110.
(183) Aboul-Fotouh, S. M.; Aboul-Gheit, A. K. *Appl. Catal., A* **2001**, *208*, 55−61.
(184) Fung, S. C. *Catal. Today* **1999**, *53*, 325−338.
(185) Foger, K.; Jaeger, H. *J. Catal.* **1985**, *92*, 64−78.
(186) Foger, K.; Jaeger, H. *Appl. Catal.* **1989**, *56*, 137−147.
(187) Dorning, T. A.; Moss, R. L. *J. Catal.* **1966**, *5*, 111−115.
(188) Sa, J.; Goguet, A.; Taylor, S. F. R.; Tiruvalam, R.; Kiely, C. J.; Nachtegaal, M.; Hutchings, G.; Hardacre, C. *Angew. Chem., Int. Ed.* **2011**, *50*, 8912−8916.
(189) Goguet, A.; Hardacre, C.; Harvey, I.; Narasimharao, K.; Saih, Y.; Sa, J. *J. Am. Chem. Soc.* **2009**, *131*, 6973−6975.
(190) Sa, J.; Taylor, S. F. R.; Daly, H.; Goguet, A.; Tiruvalam, R.; He, Q.; Kiely, C. J.; Hutchings, G. J.; Hardacre, C. *ACS Catal.* **2012**, *2*, 552−560.
(191) Li, F.; Qian, Q.; Yan, F.; Yuan, G. *Mater. Chem. Phys.* **2008**, *107*, 310−316.
(192) Zoeller, J. R.; Singleton, A. H.; Tustin, G. C.; Carver, D. L. US Patent 6,506,933, 2003.
(193) Zoeller, J. R.; Singleton, A. H.; Tustin, G. C.; Carver, D. L. US Patent 6,509,293, 2003.
(194) Morgan, K.; Burch, R.; Daous, M.; Delgado, J.-J.; Goguet, A.; Hardacre, C.; Petrov, L. A.; Rooney, D. W. *Catal. Struct. React.* **2015**, DOI: 10.1179/2055075815Y.0000000005.
(195) Chu, Y. F.; Ruckenstein, E. *J. Catal.* **1978**, *55*, 281−298.
(196) Lamber, R.; Romanowski, W. *J. Catal.* **1987**, *105*, 213−226.
(197) Sushumna, I.; Ruckenstein, E. *J. Catal.* **1987**, *108*, 77−96.
(198) Gollob, R.; Dadyburjor, D. B. *J. Catal.* **1981**, *68*, 473−486.

DOI: 10.1021/acscatal.5b00535
ACS Catal. 2015, 5, 3430−3445